Electronic Supplementary Material (ESI) for Analytical Methods

A quantitative assessment of the chemical variation in food grade polyethylene cling film, a common wrapping material for illicit drugs, using attenuated total reflection-Fourier transform infrared spectroscopy

Supporting information

Stephen W. Holman[1¤*], Trevor F. Emmett[1] and Michael D. Cole[1]

[1] Department of Life Sciences, Anglia Ruskin University, Cambridge, CB1 1PT, UK

¤ Current address: Michael Barber Centre for Mass Spectrometry, Manchester Interdisciplinary Centre, The University of Manchester, 131 Princess Street, Manchester, M1 7DN, UK

*Address correspondence to:

Stephen W. Holman
Michael Barber Centre for Mass Spectrometry
Manchester Interdisciplinary Biocentre
The University of Manchester
131 Princess Street
Manchester
M1 7DN
UK

E-mail: stephen.holman@manchester.ac.uk

Tel: +44 161 306 4821

Fax: +44 161 306 8918

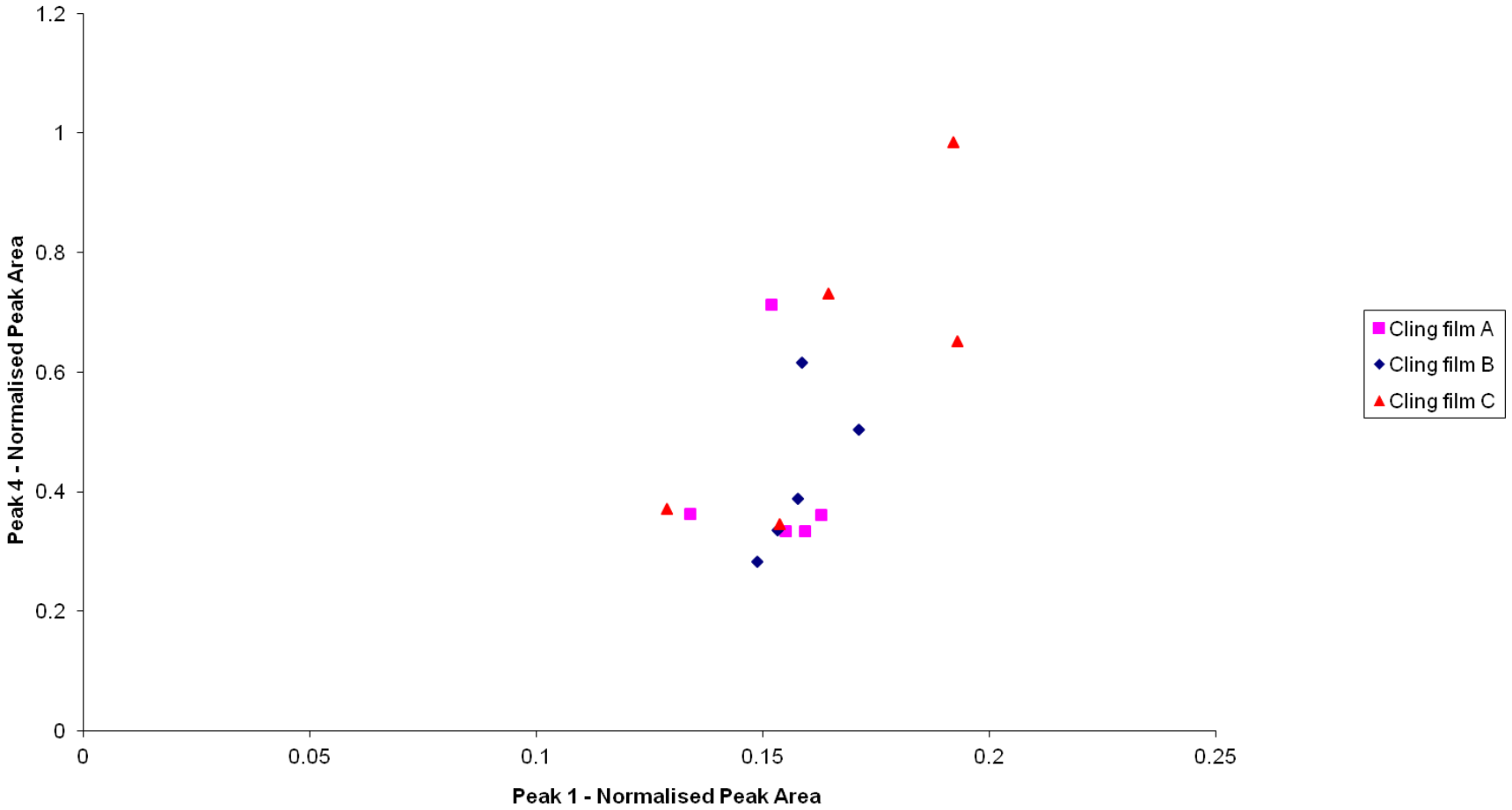

Figure S1 Bivariate plot of the normalised peak areas for peaks 1 and 4 from the five high resolution IR spectra recorded for cling films A, B and C

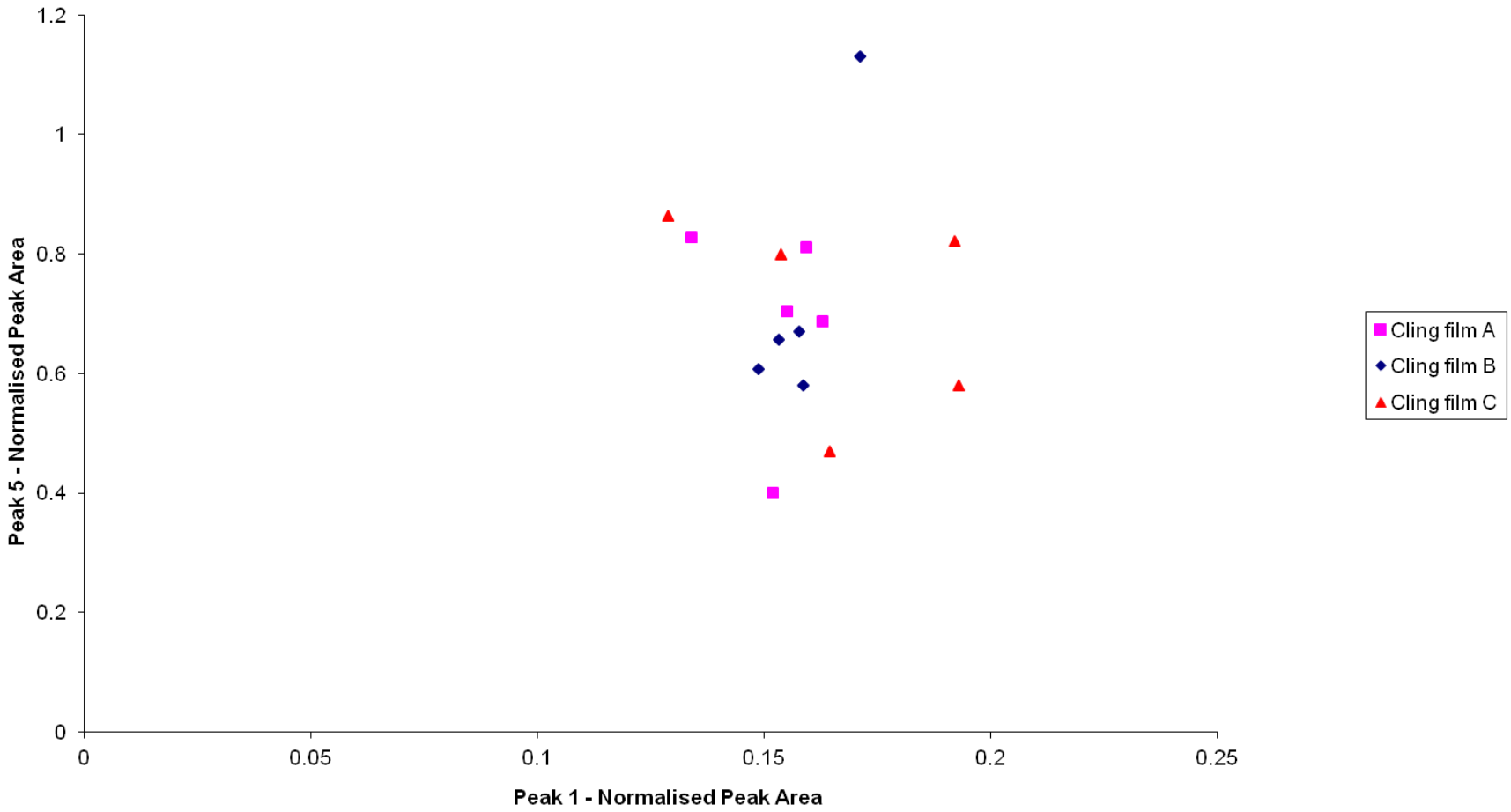

Figure S2 Bivariate plot of the normalised peak areas for peaks 1 and 5 from the five high resolution IR spectra recorded for cling films A, B and C

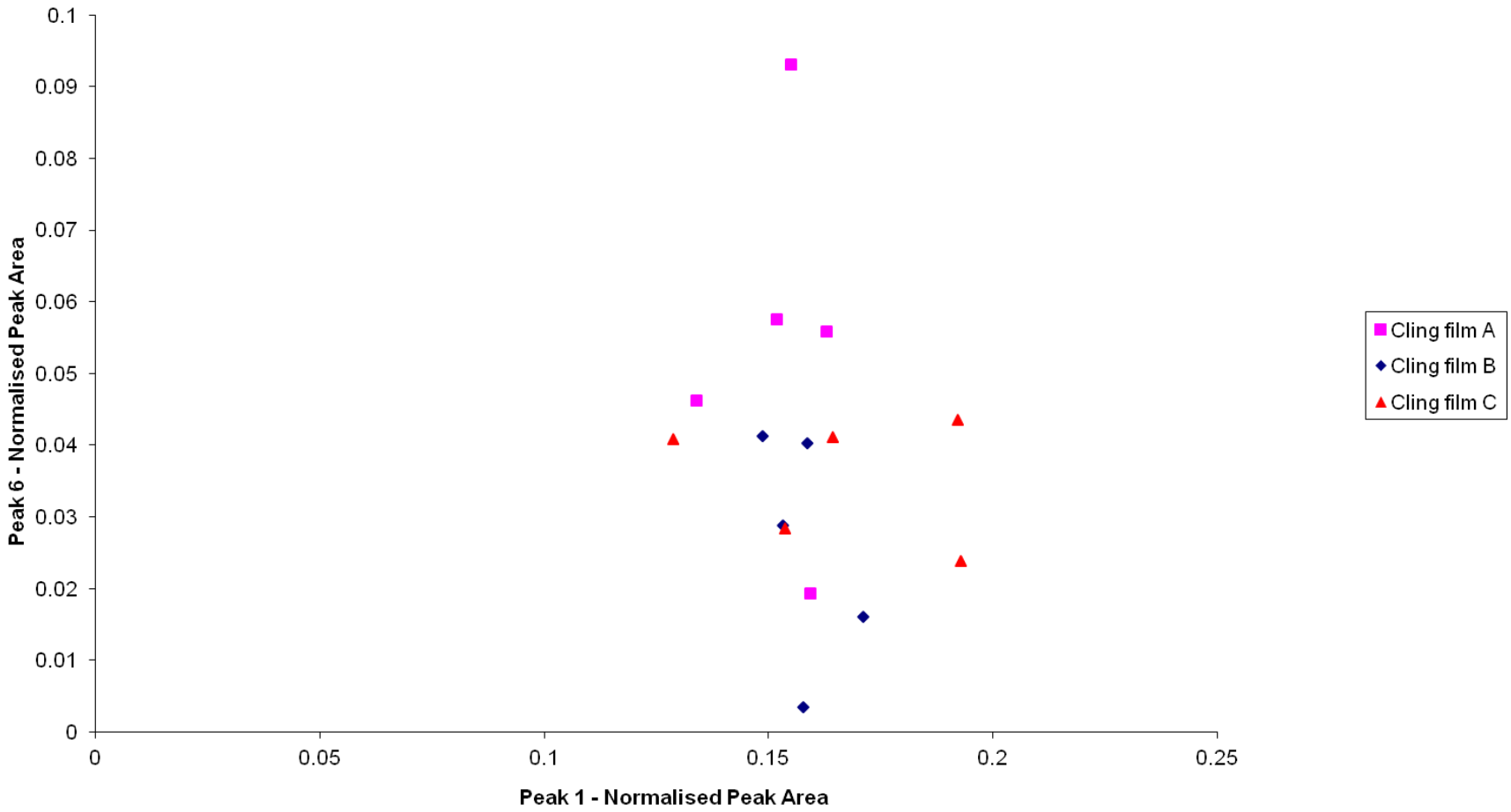

Figure S3 Bivariate plot of the normalised peak areas for peaks 1 and 6 from the five high resolution IR spectra recorded for cling films A, B and C

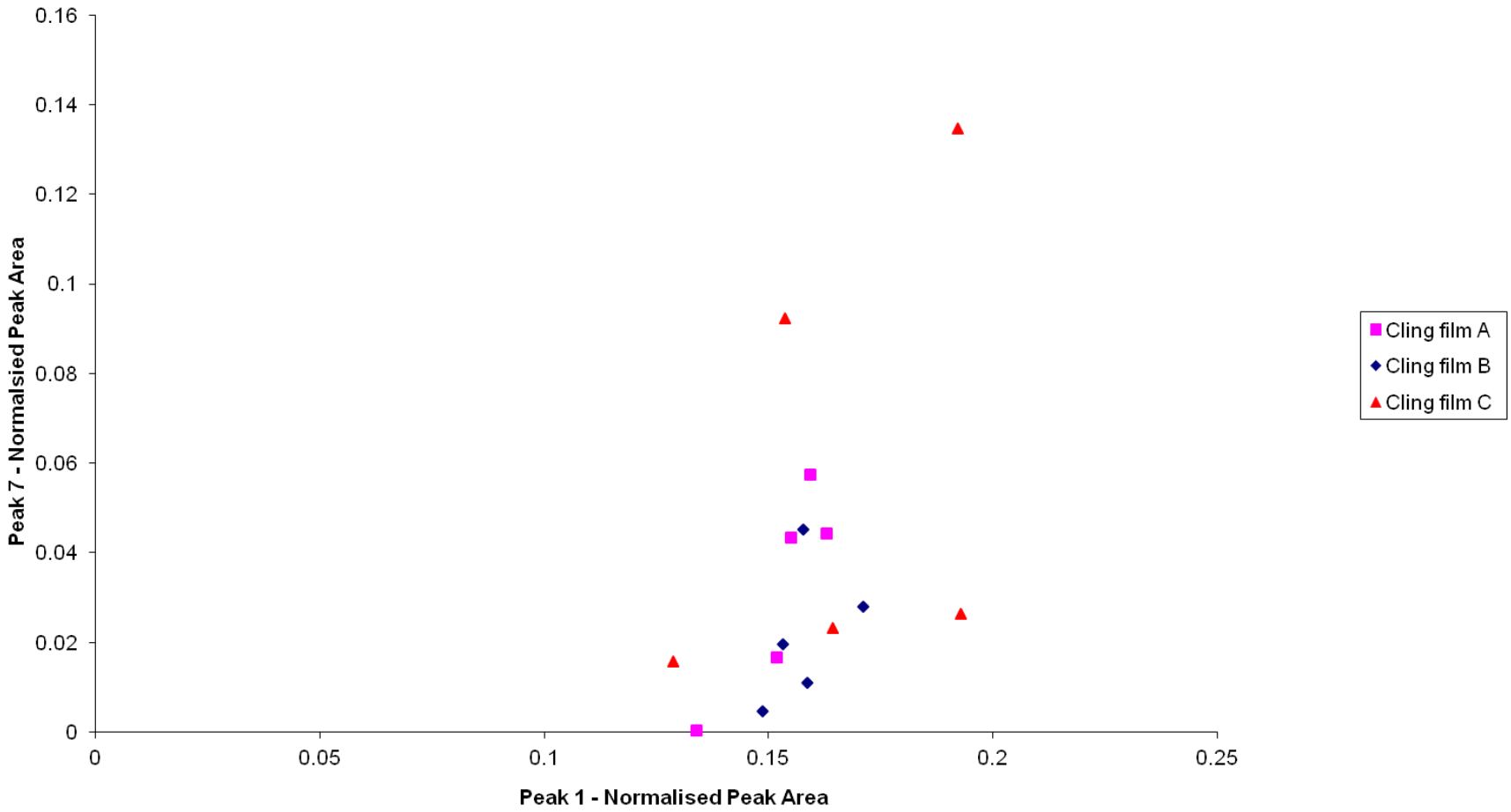

Figure S4 Bivariate plot of the normalised peak areas for peaks 1 and 7 from the five high resolution IR spectra recorded for cling films A, B and C

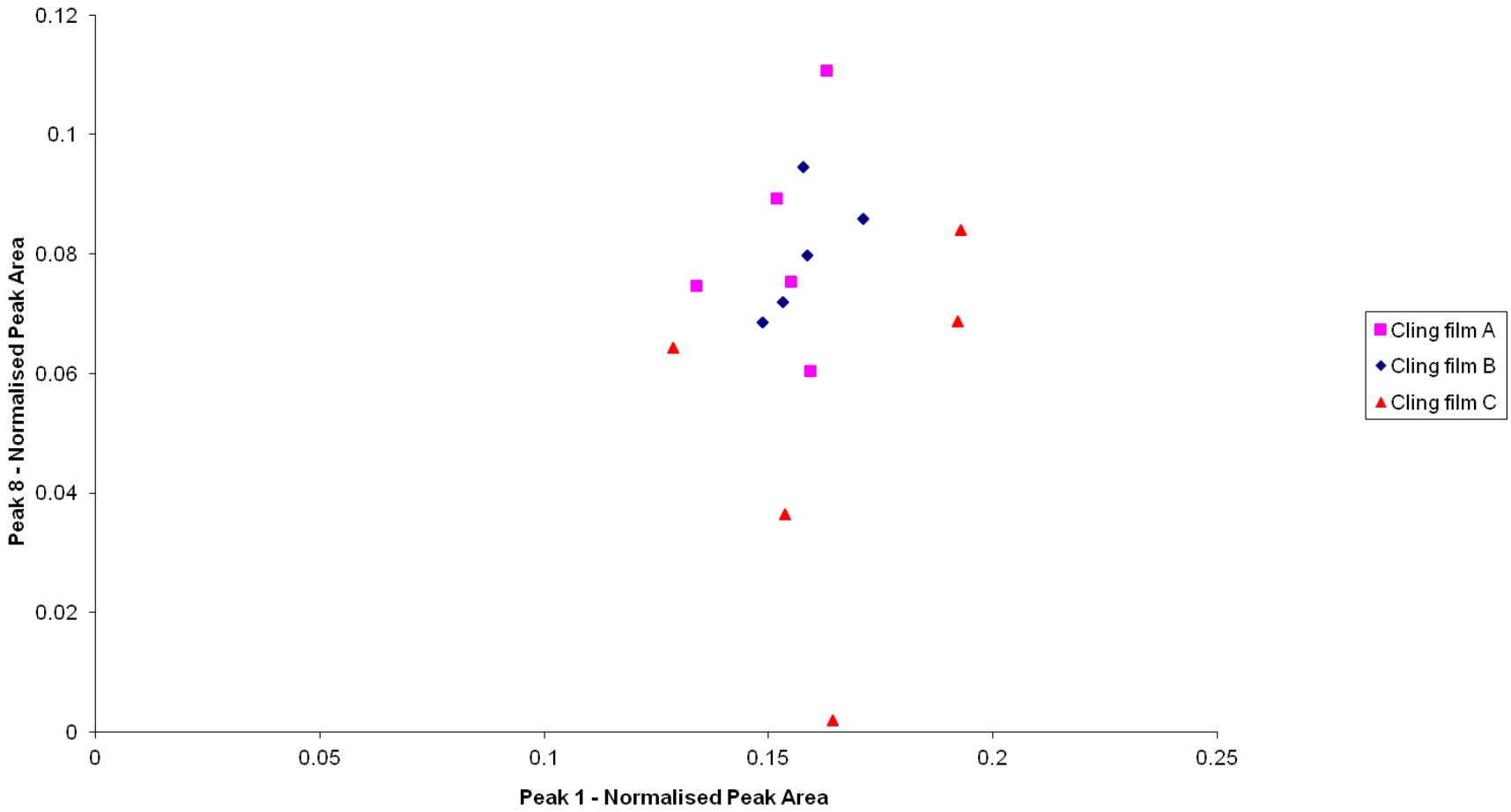

Figure S5 Bivariate plot of the normalised peak areas for peaks 1 and 8 from the five high resolution IR spectra recorded for cling films A, B and C

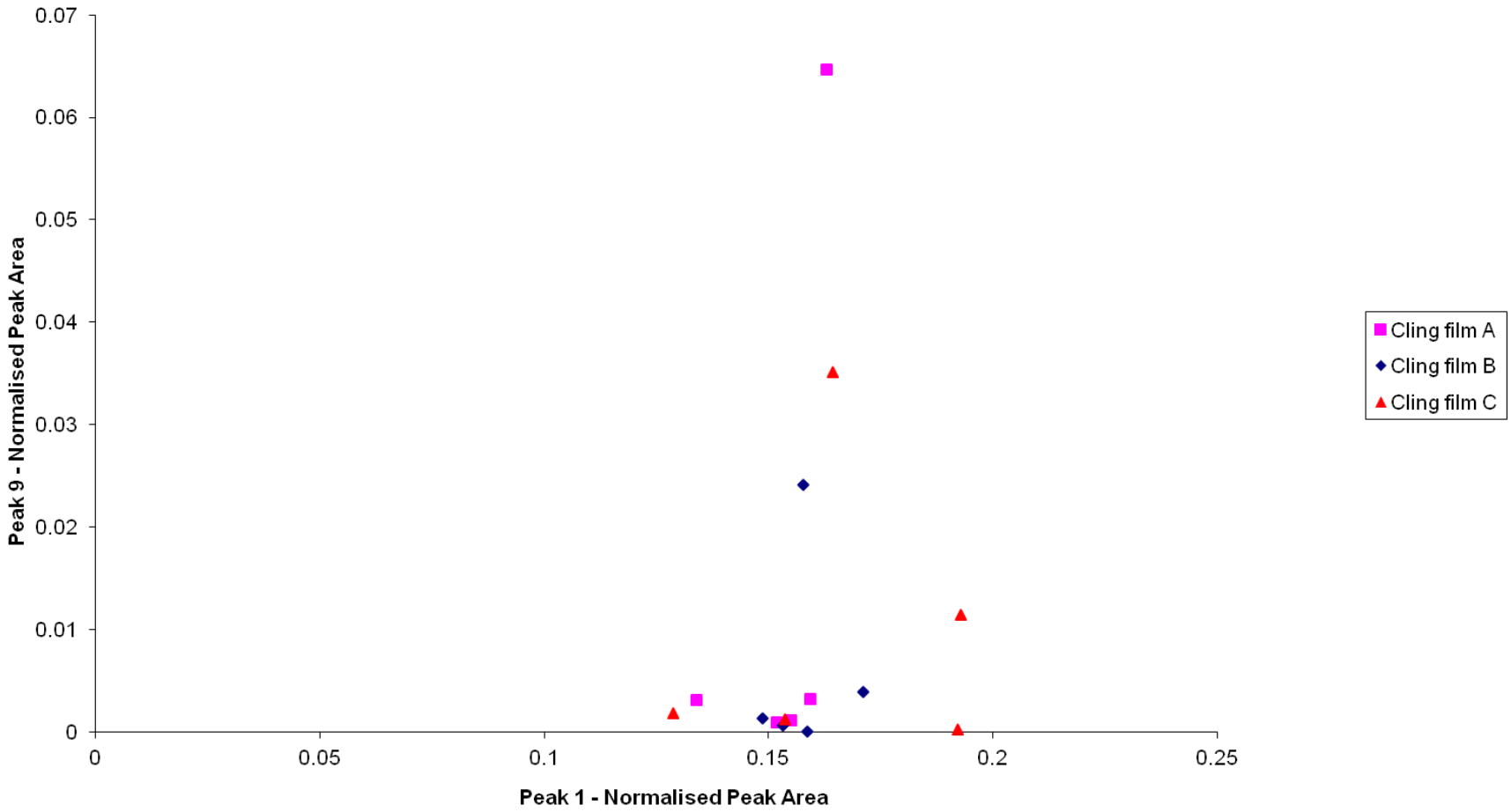

Figure S6 Bivariate plot of the normalised peak areas for peaks 1 and 9 from the five high resolution IR spectra recorded for cling films A, B and C

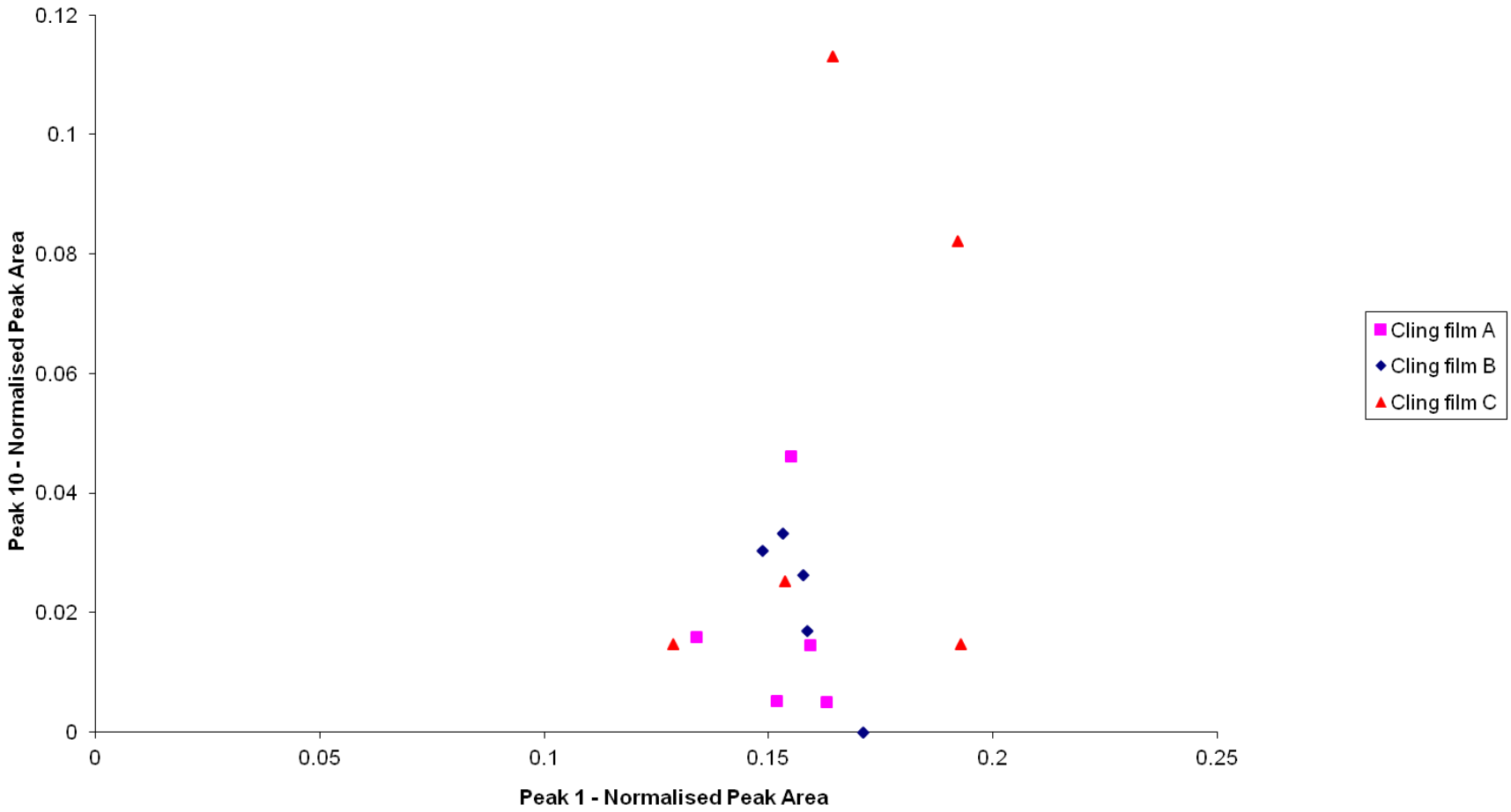

Figure S7 Bivariate plot of the normalised peak areas for peaks 1 and 10 from the five high resolution IR spectra recorded for cling films A, B and C

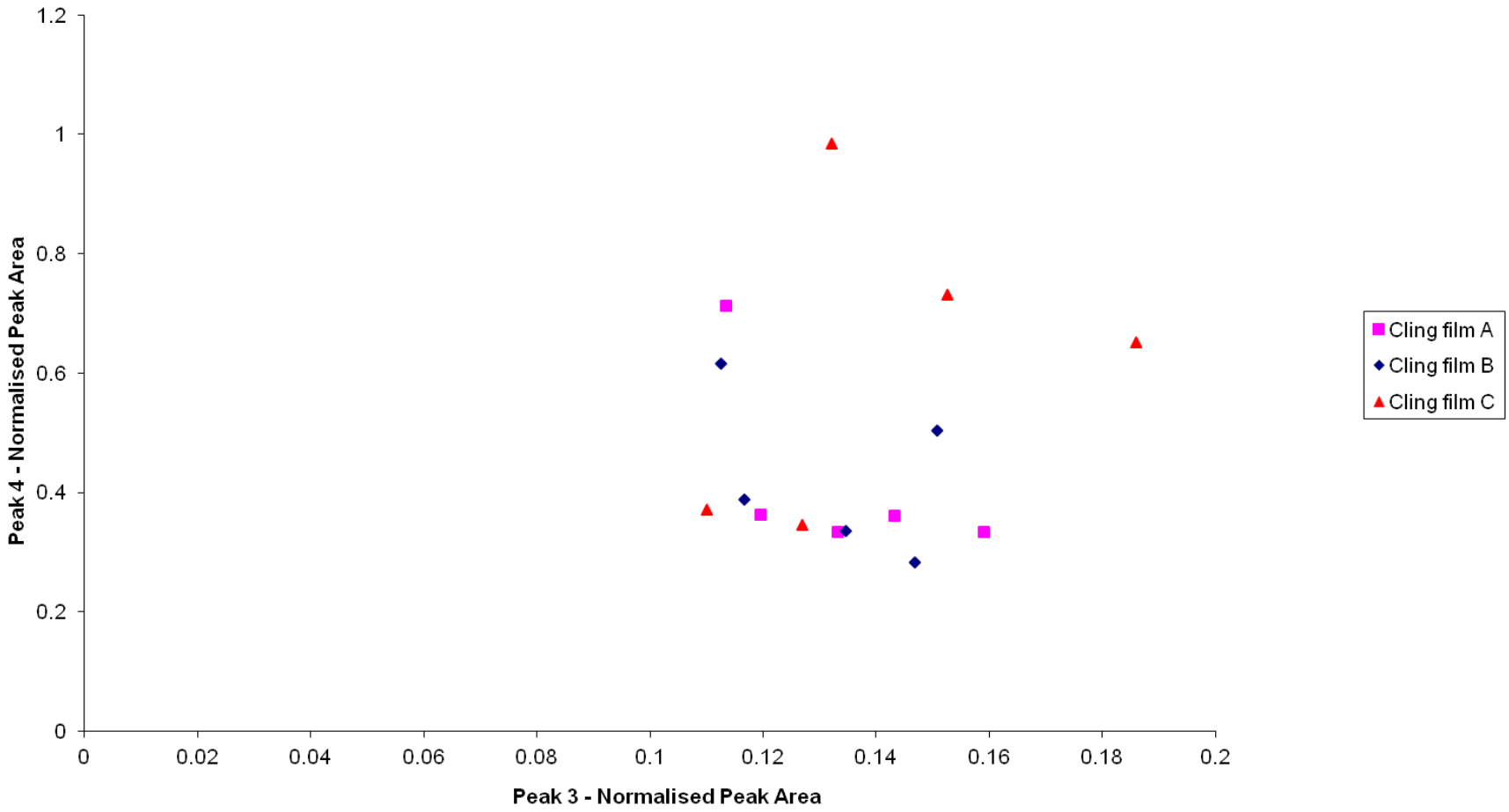

Figure S8 Bivariate plot of the normalised peak areas for peaks 3 and 4 from the five high resolution IR spectra recorded for cling films A, B and C

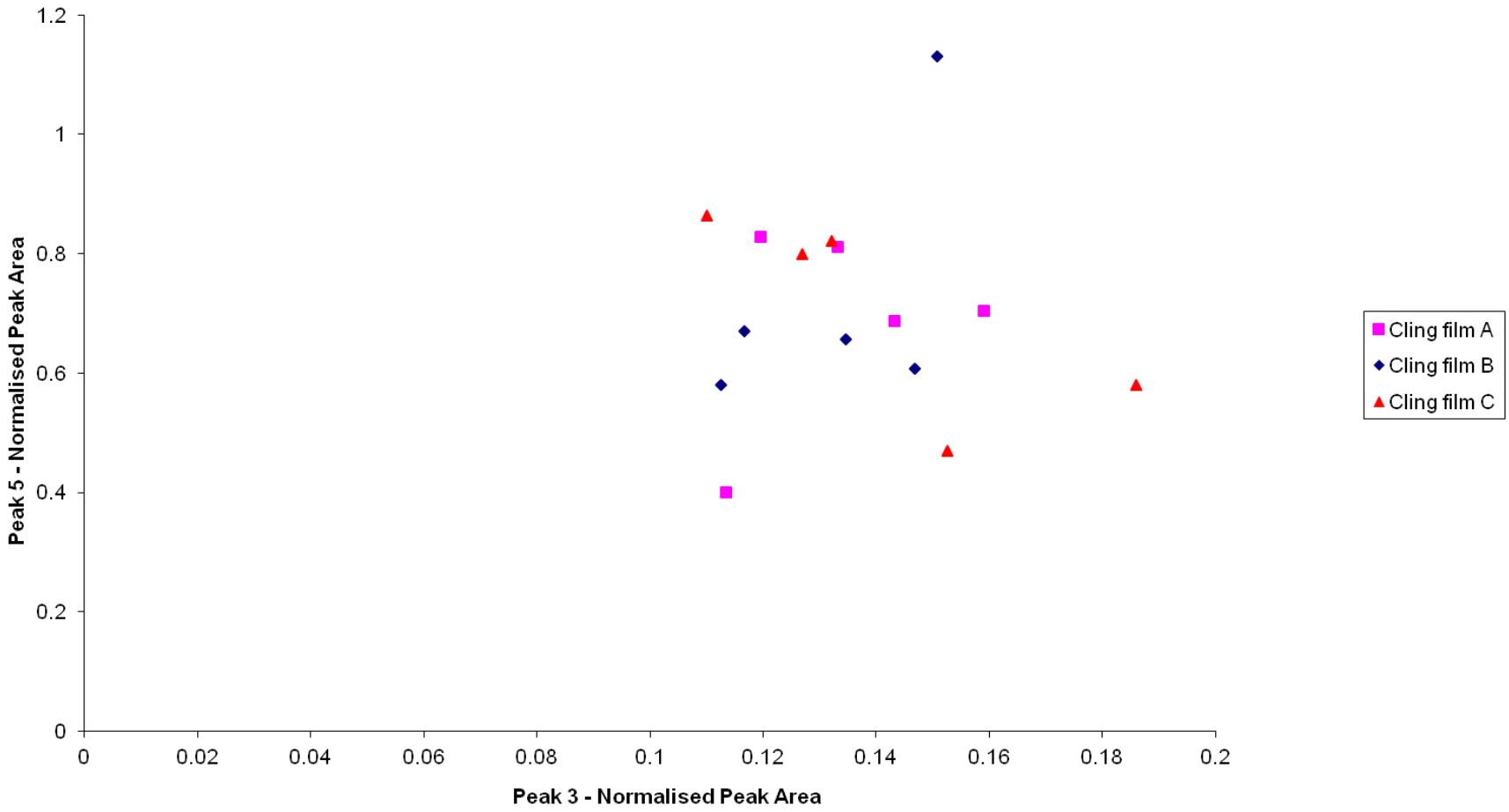

Figure S9 Bivariate plot of the normalised peak areas for peaks 3 and 5 from the five high resolution IR spectra recorded for cling films A, B and C

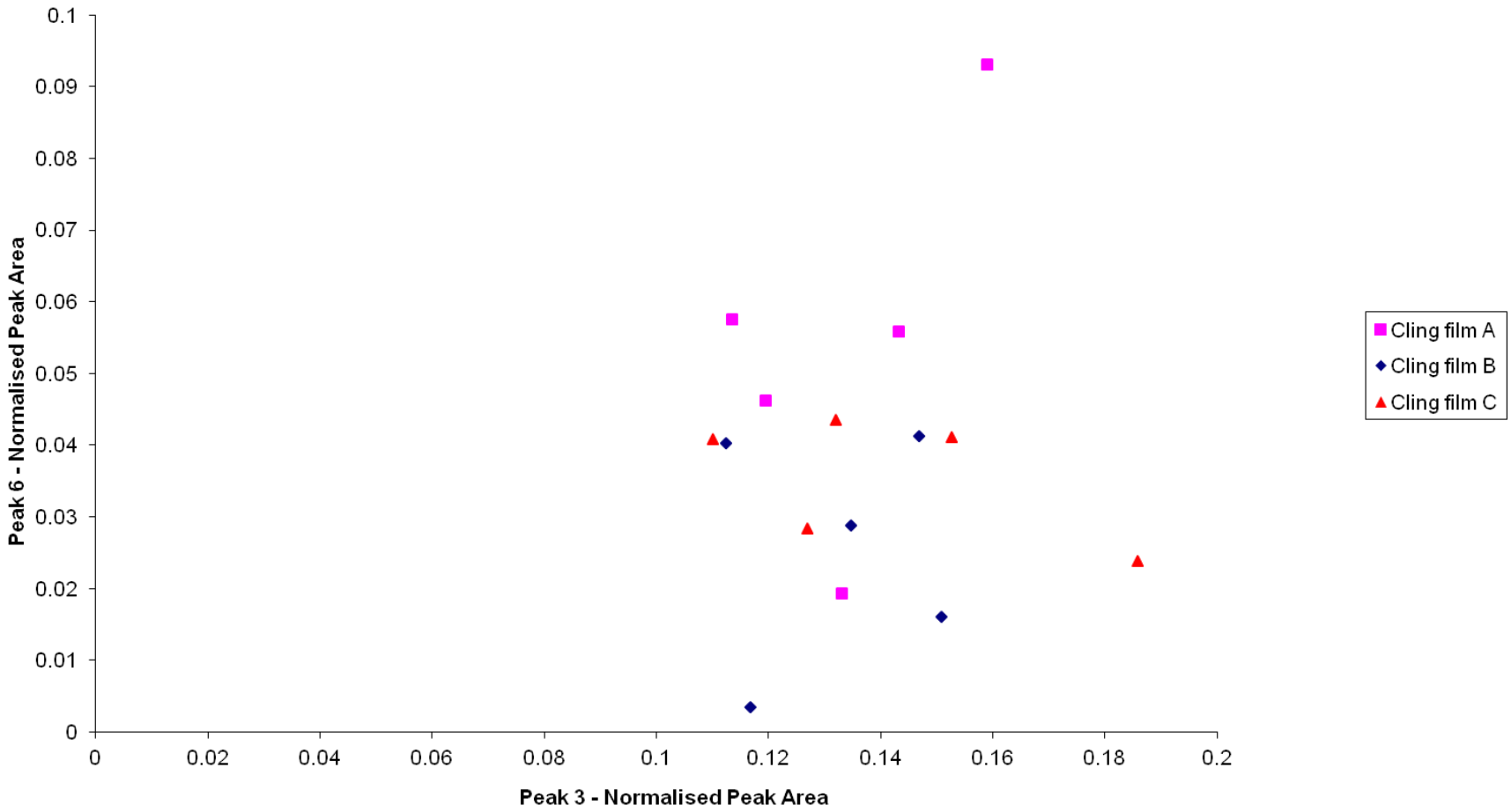

Figure S10 Bivariate plot of the normalised peak areas for peaks 3 and 6 from the five high resolution IR spectra recorded for cling films A, B and C

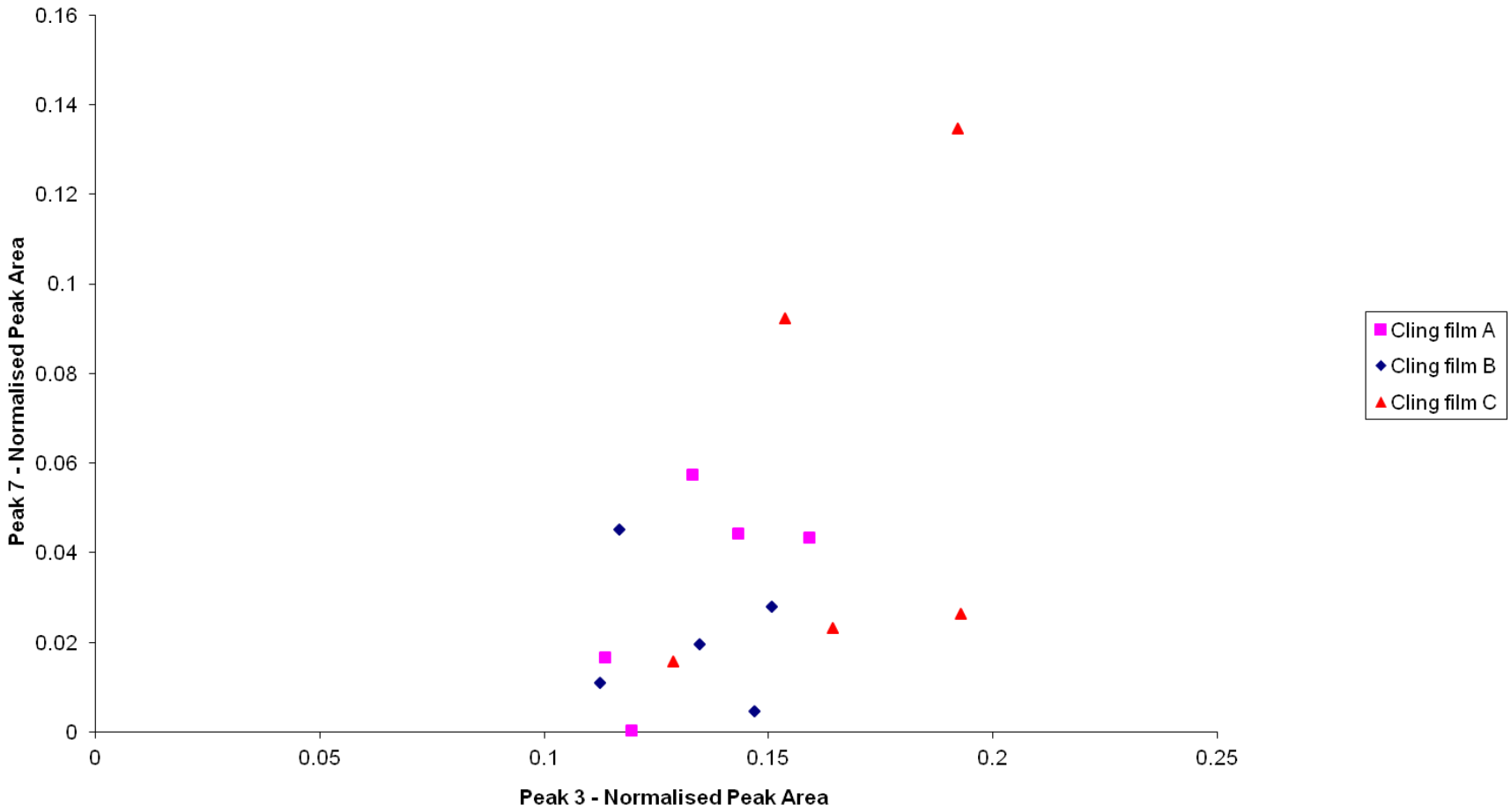

Figure S11 Bivariate plot of the normalised peak areas for peaks 3 and 7 from the five high resolution IR spectra recorded for cling films A, B and C

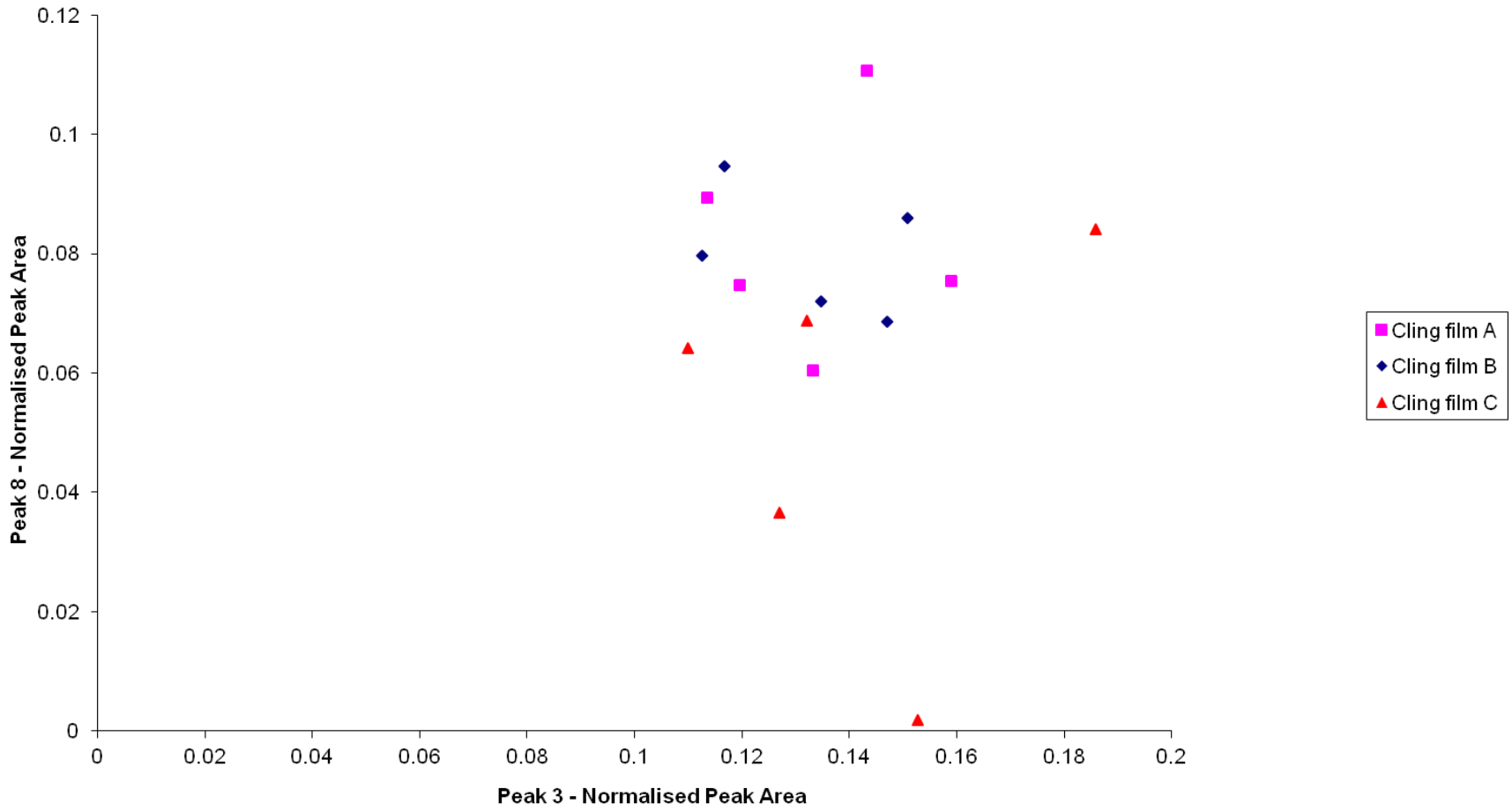

Figure S12 Bivariate plot of the normalised peak areas for peaks 3 and 8 from the five high resolution IR spectra recorded for cling films A, B and C

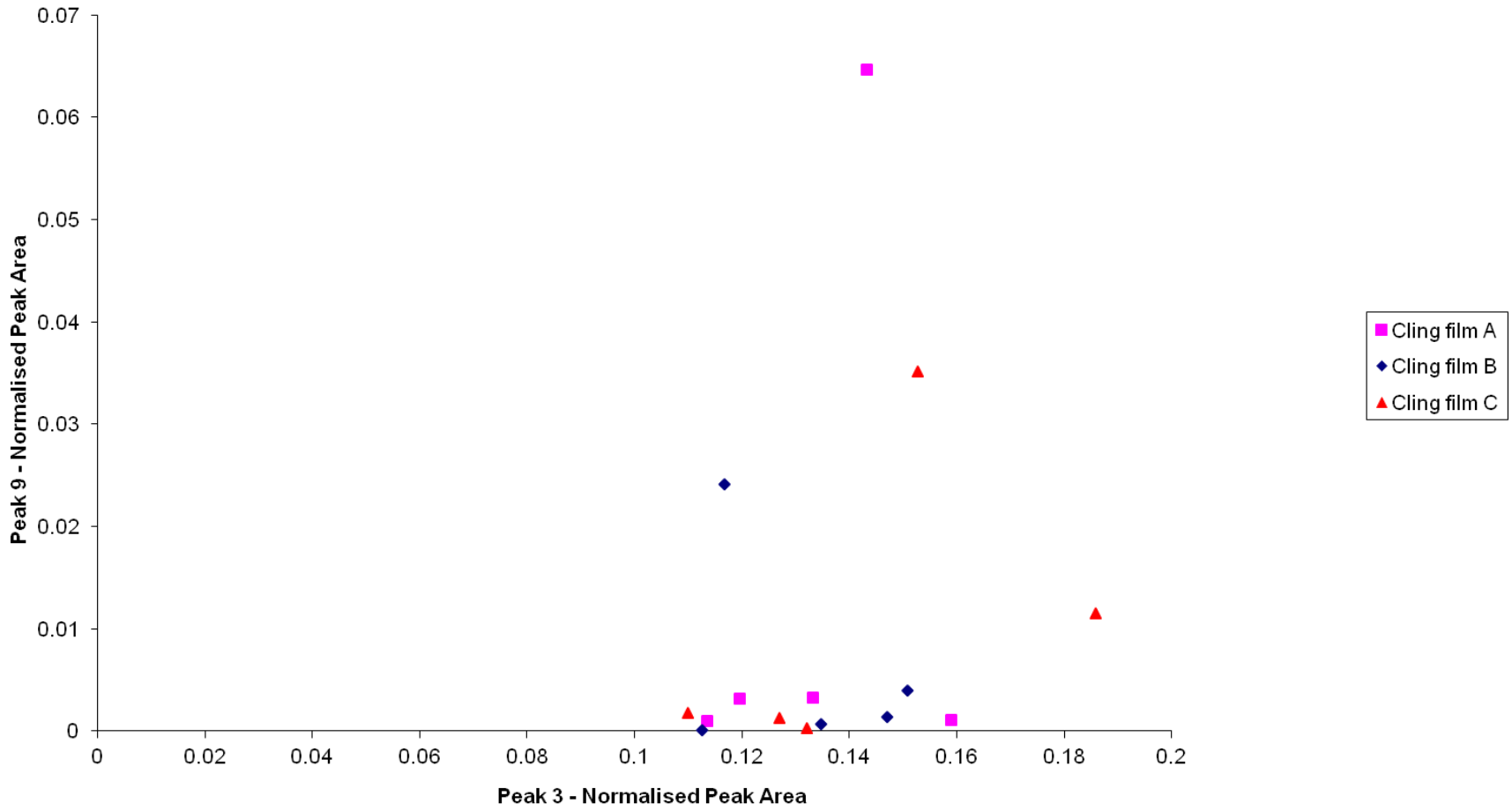

Figure S13 Bivariate plot of the normalised peak areas for peaks 3 and 9 from the five high resolution IR spectra recorded for cling films A, B and C

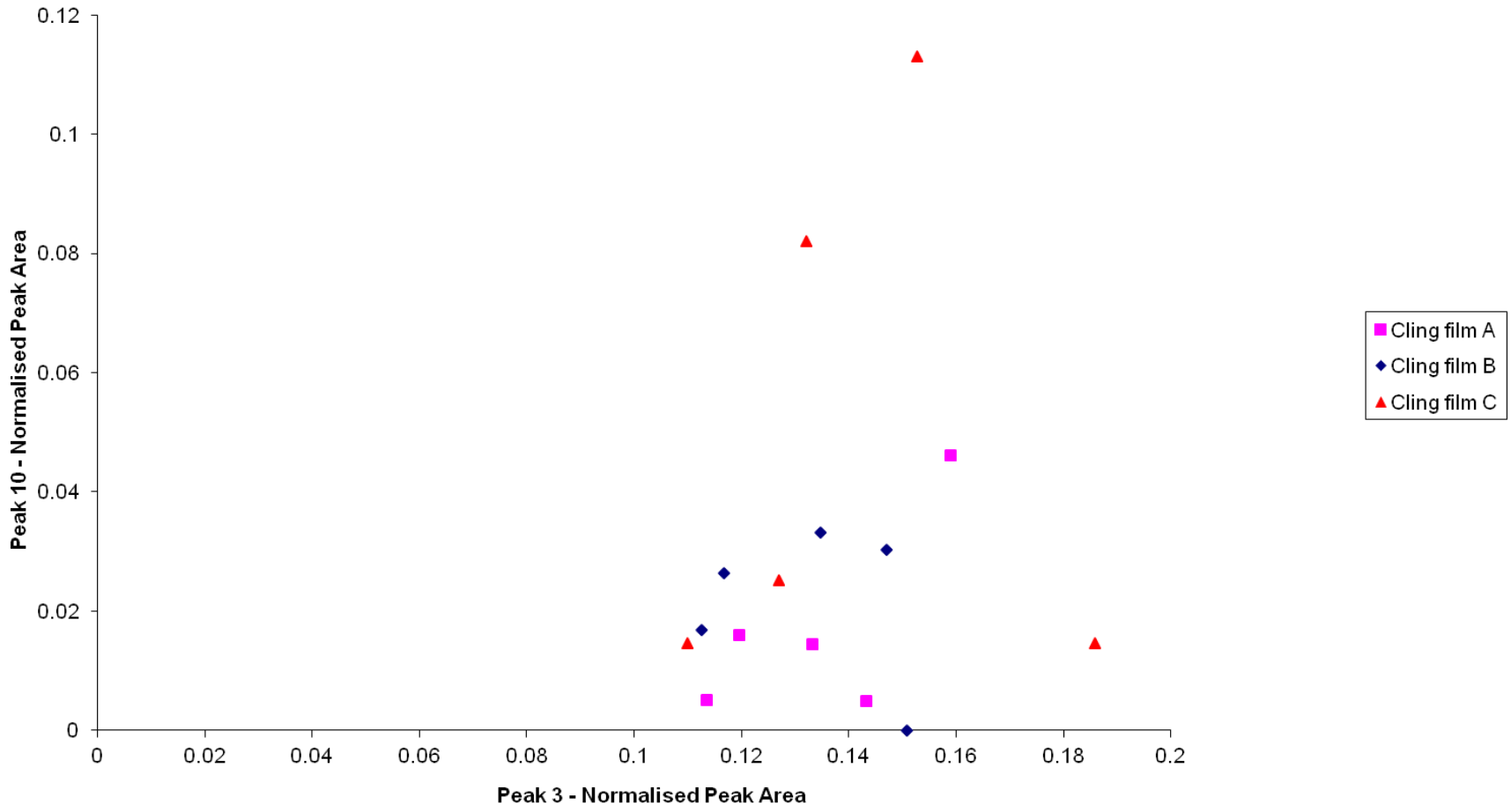

Figure S14 Bivariate plot of the normalised peak areas for peaks 3 and 10 from the five high resolution IR spectra recorded for cling films A, B and C

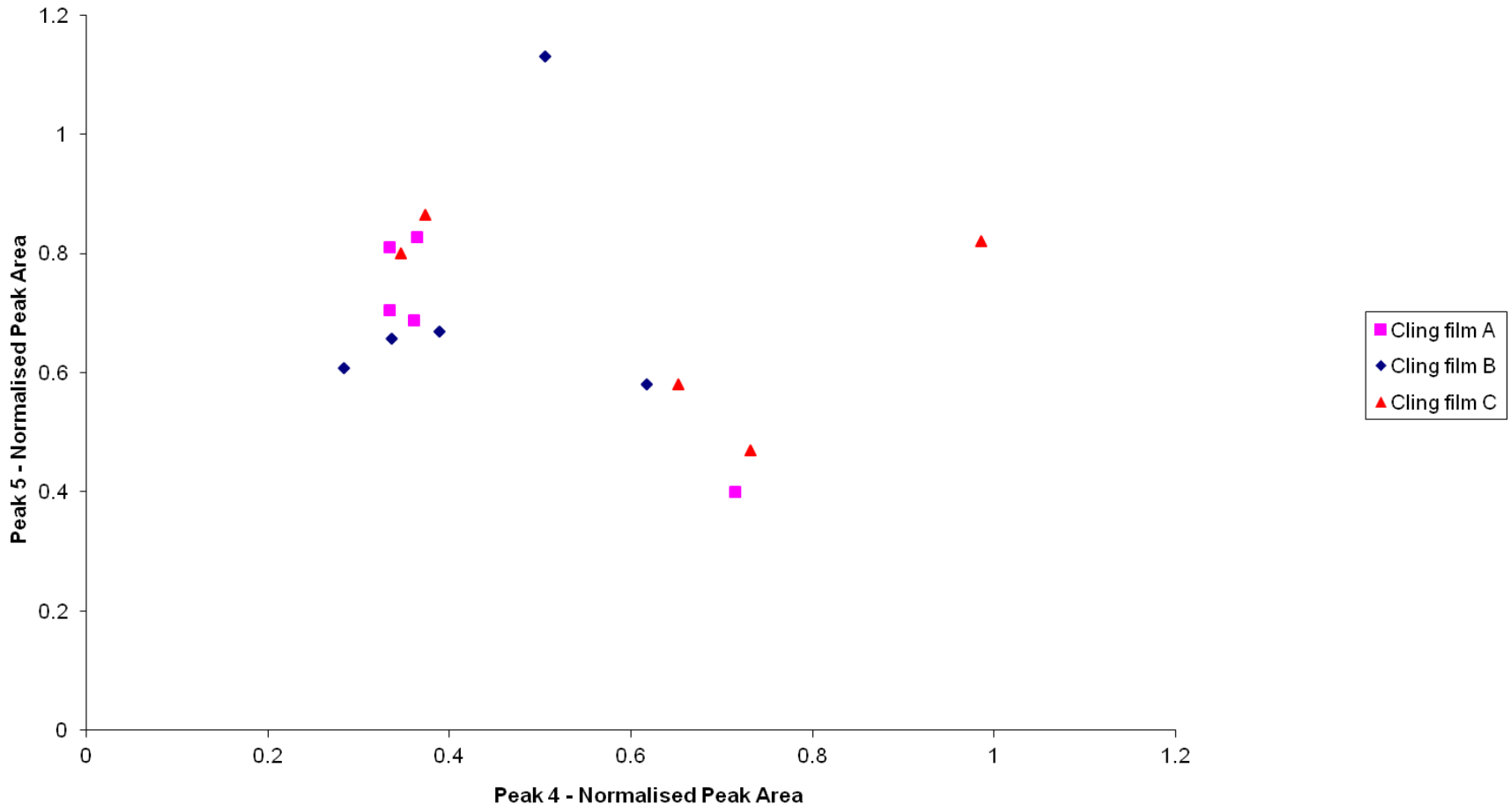

Figure S15 Bivariate plot of the normalised peak areas for peaks 4 and 5 from the five high resolution IR spectra recorded for cling films A, B and C

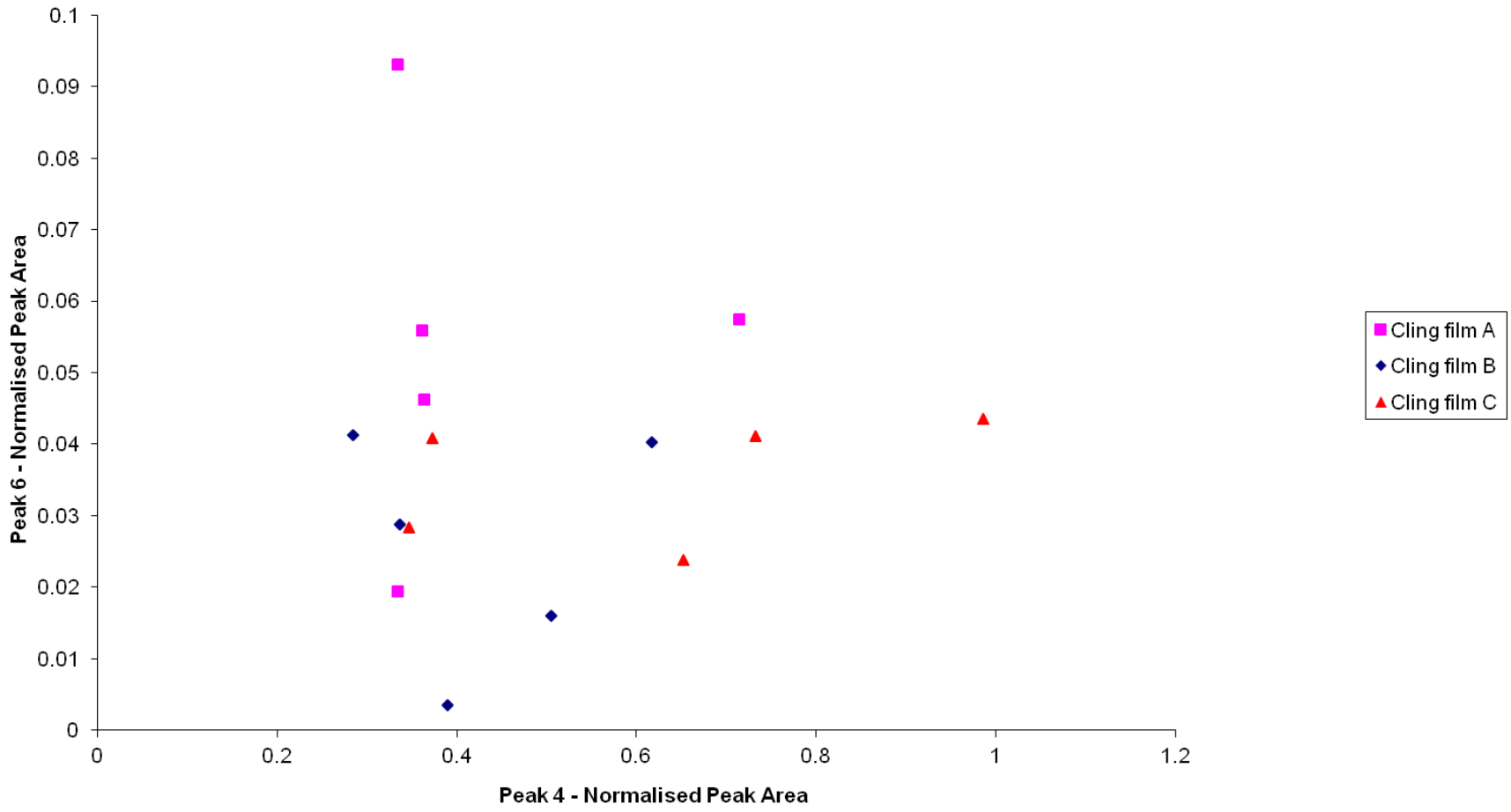

Figure S16 Bivariate plot of the normalised peak areas for peaks 4 and 6 from the five high resolution IR spectra recorded for cling films A,B and C

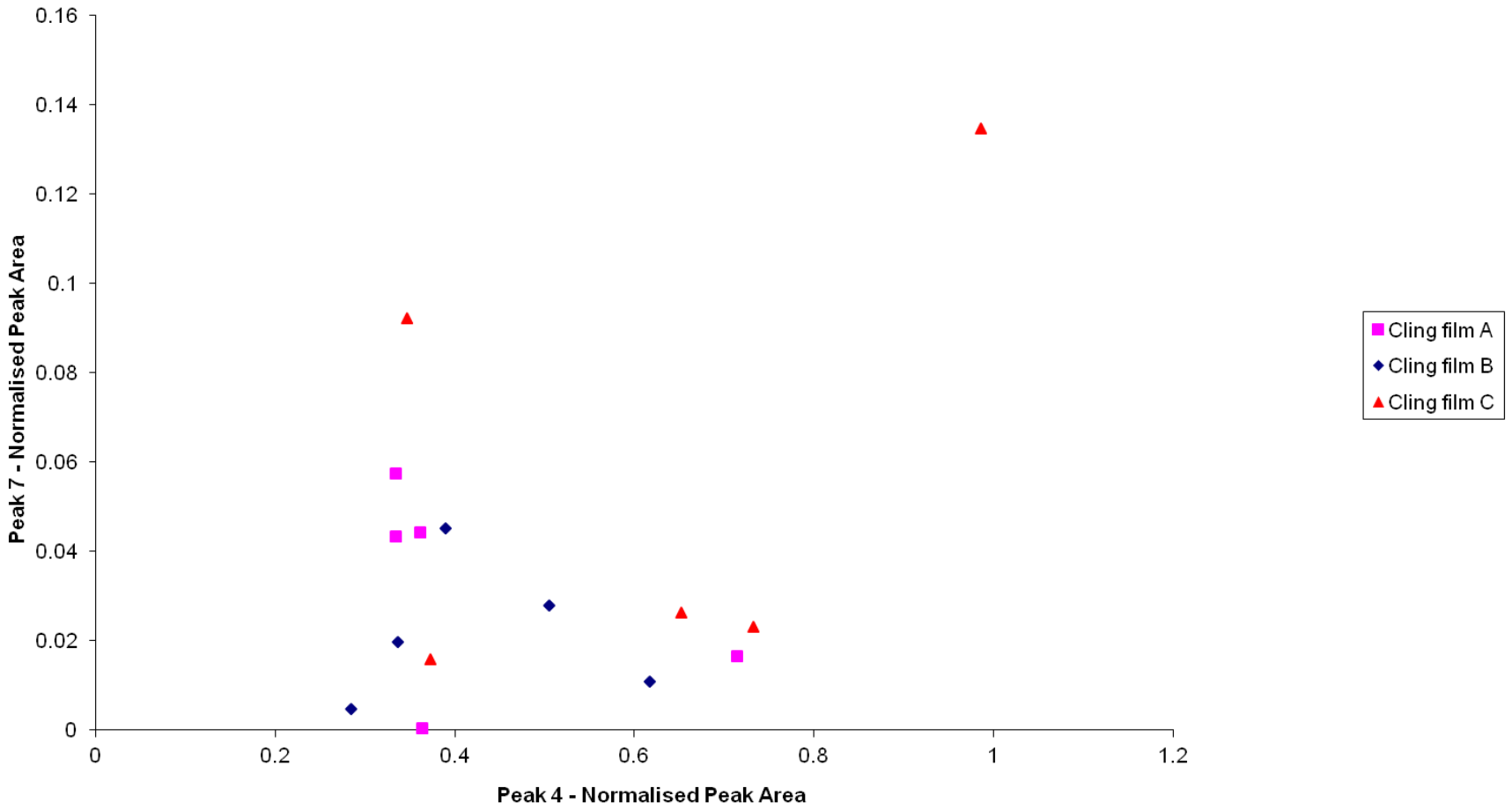

Figure S17 Bivariate plot of the normalised peak areas for peaks 4 and 7 from the five high resolution IR spectra recorded for cling films A,B and C

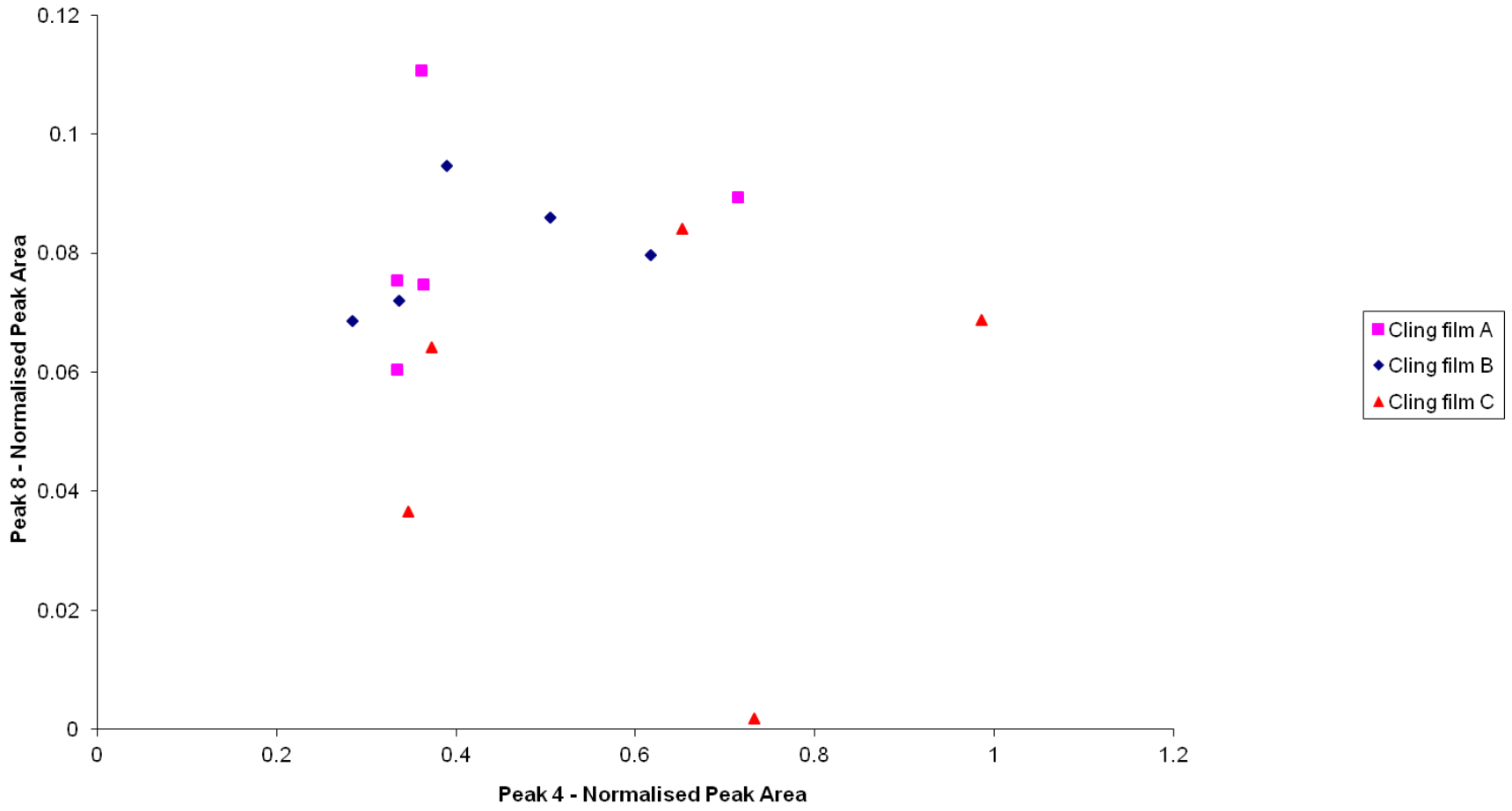

Figure S18 Bivariate plot of the normalised peak areas for peaks 4 and 8 from the five high resolution IR spectra recorded for cling films A,B and C

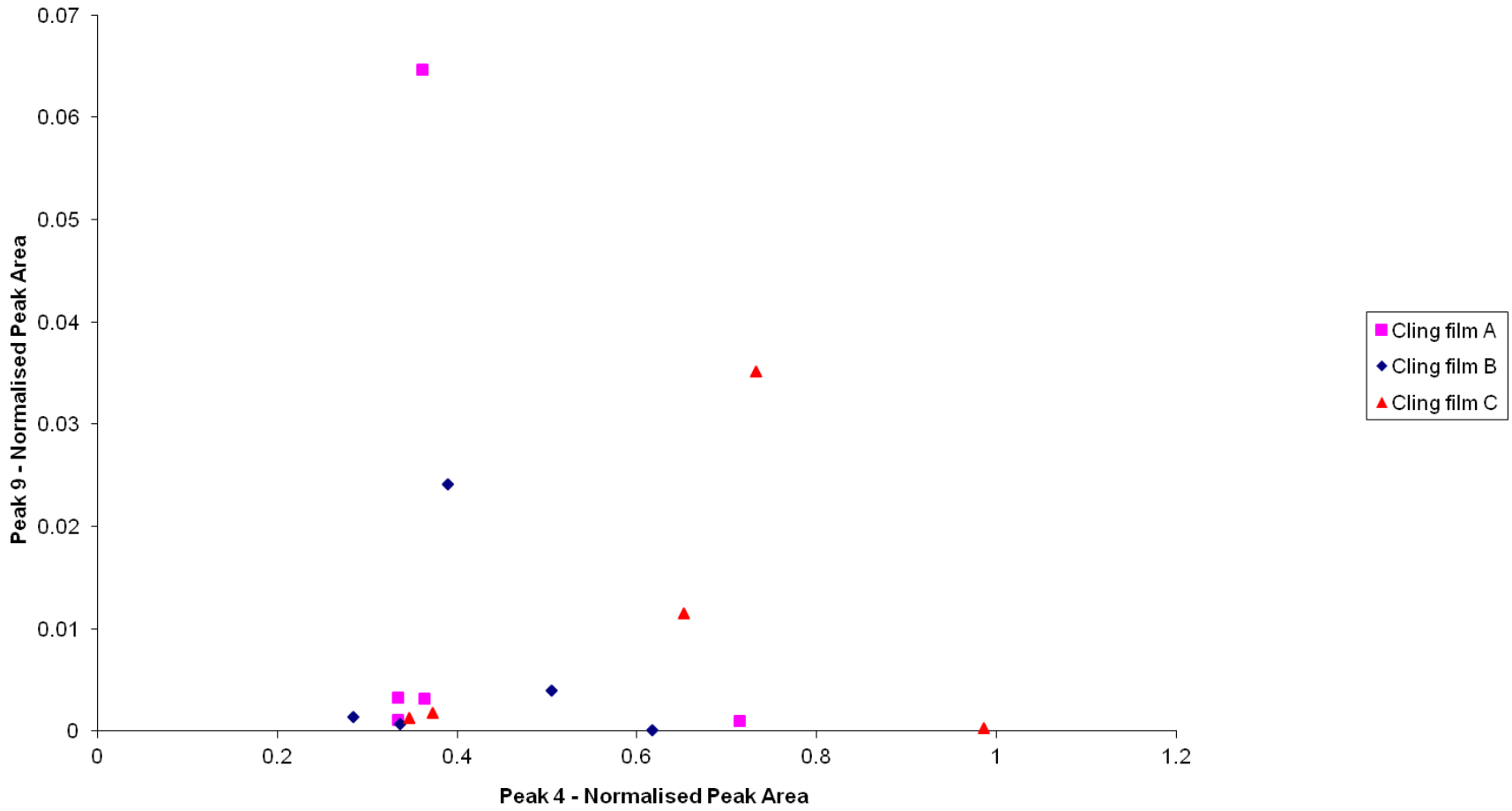

Figure S19 Bivariate plot of the normalised peak areas for peaks 4 and 9 from the five high resolution IR spectra recorded for cling films A,B and C

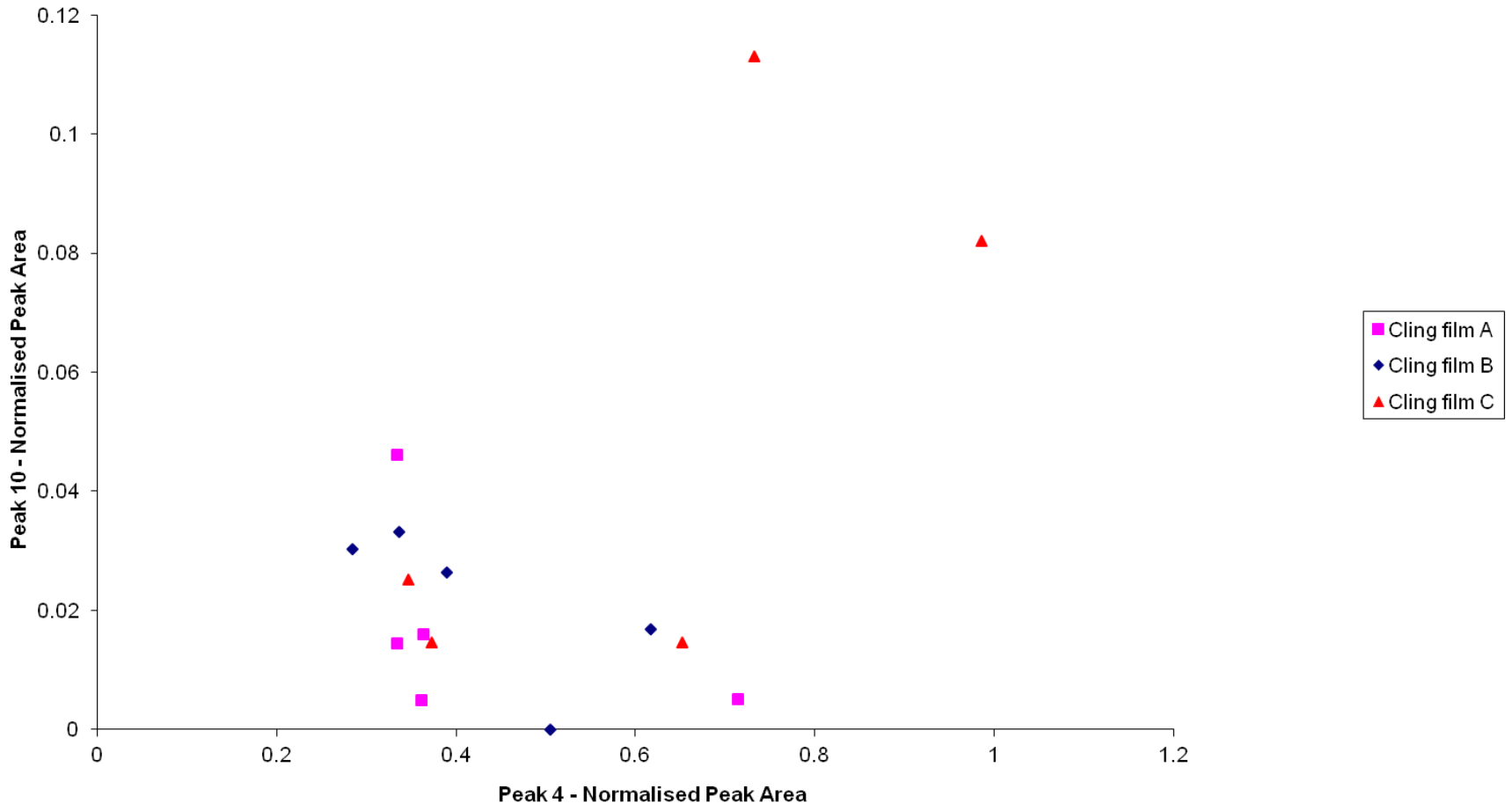

Figure S20 Bivariate plot of the normalised peak areas for peaks 4 and 10 from the five high resolution IR spectra recorded for cling films A,B and C

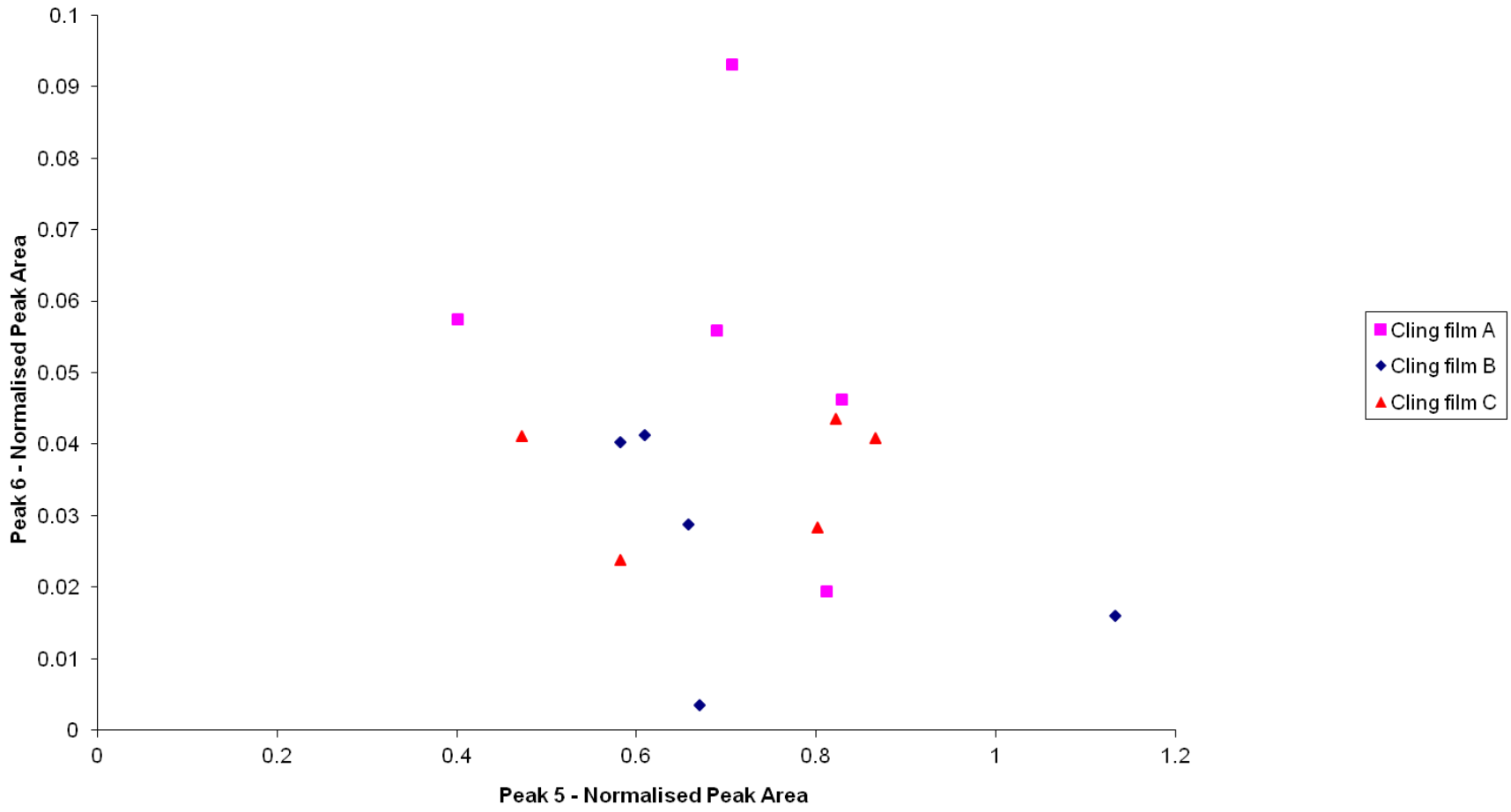

Figure S21 Bivariate plot of the normalised peak areas for peaks 5 and 6 from the five high resolution IR spectra recorded for cling films A, B and C

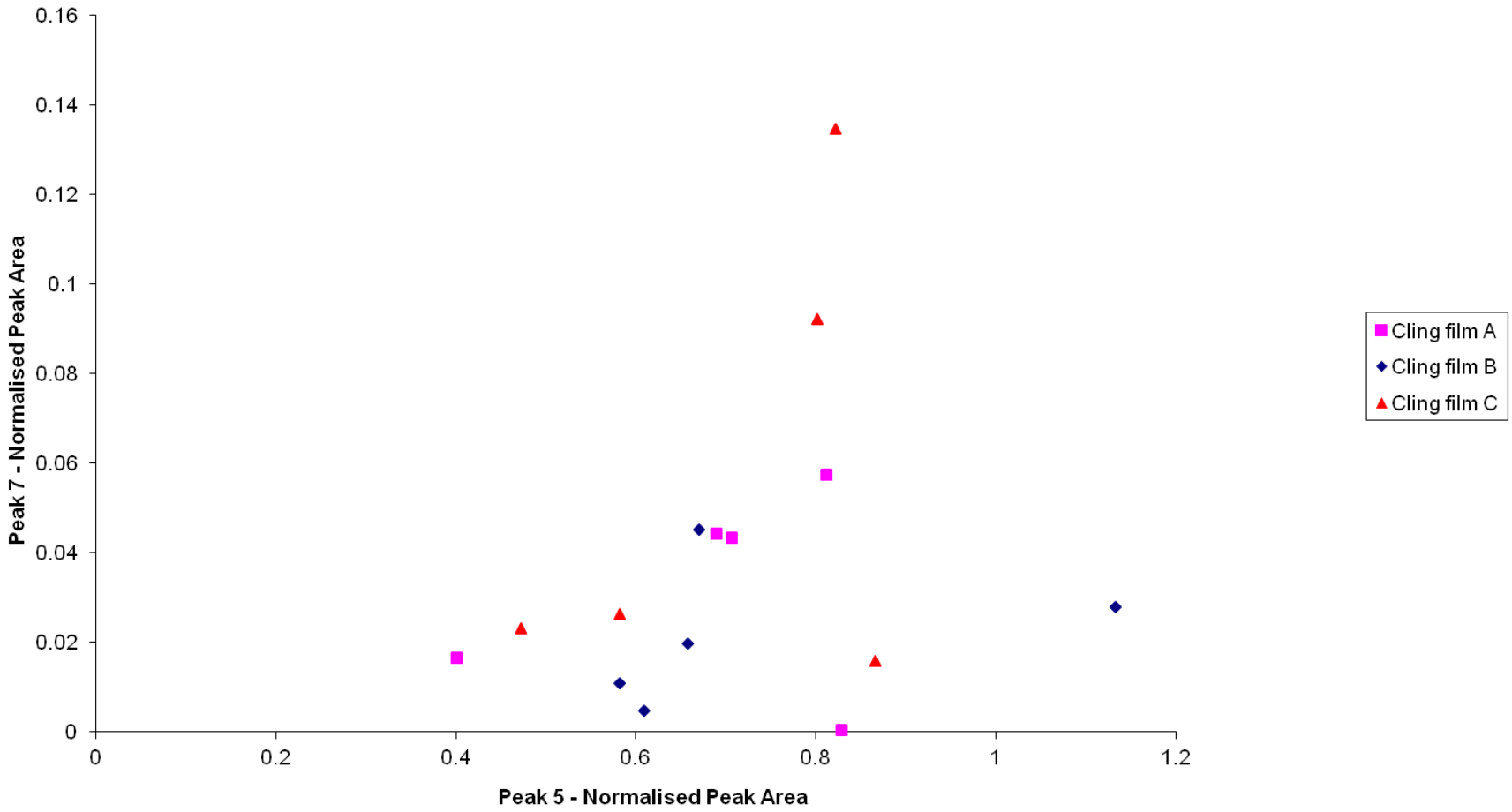

Figure S22 Bivariate plot of the normalised peak areas for peaks 5 and 7 from the five high resolution IR spectra recorded for cling films A, B and C

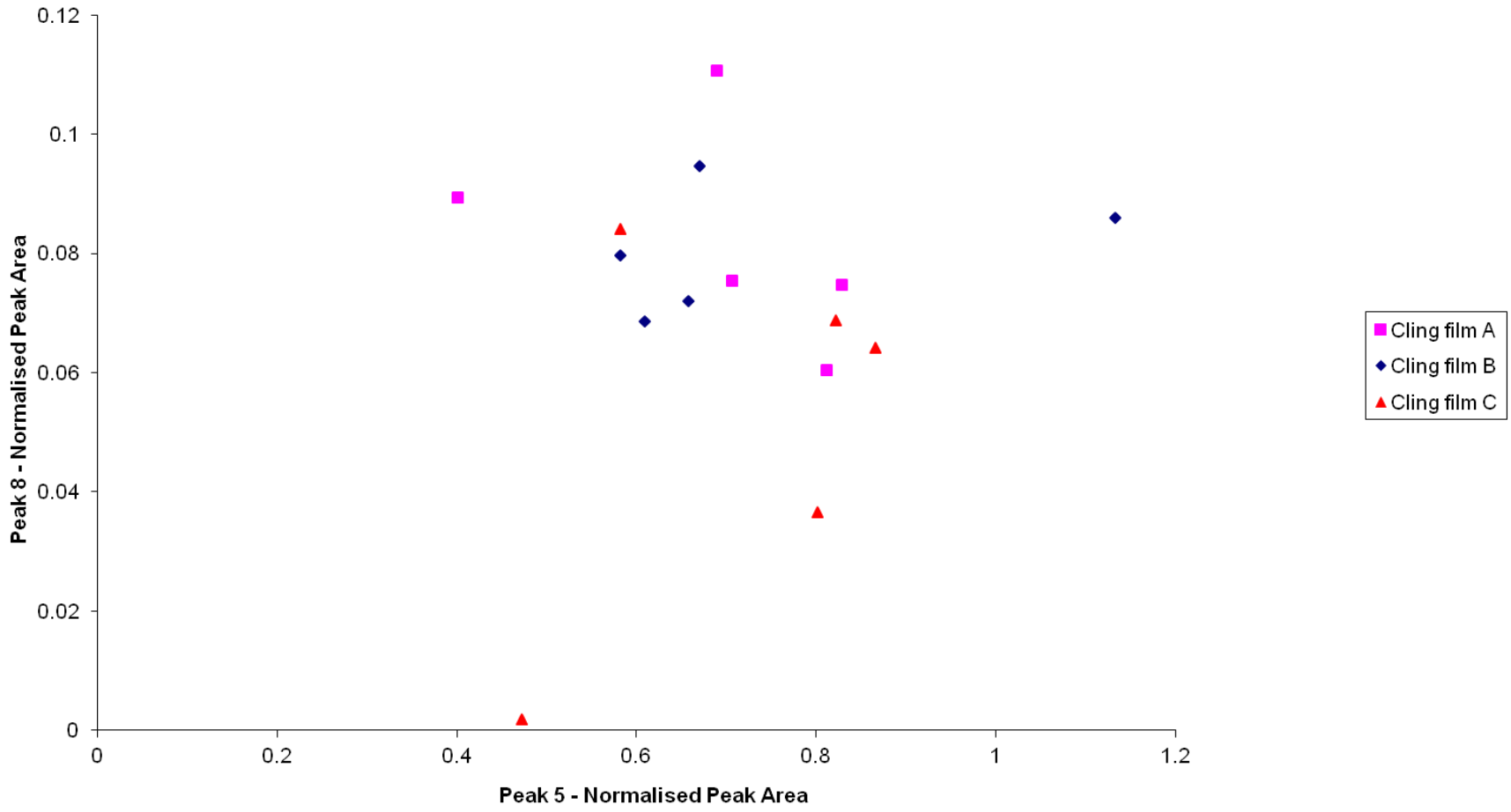

Figure S23 Bivariate plot of the normalised peak areas for peaks 5 and 8 from the five high resolution IR spectra recorded for cling films A, B and C

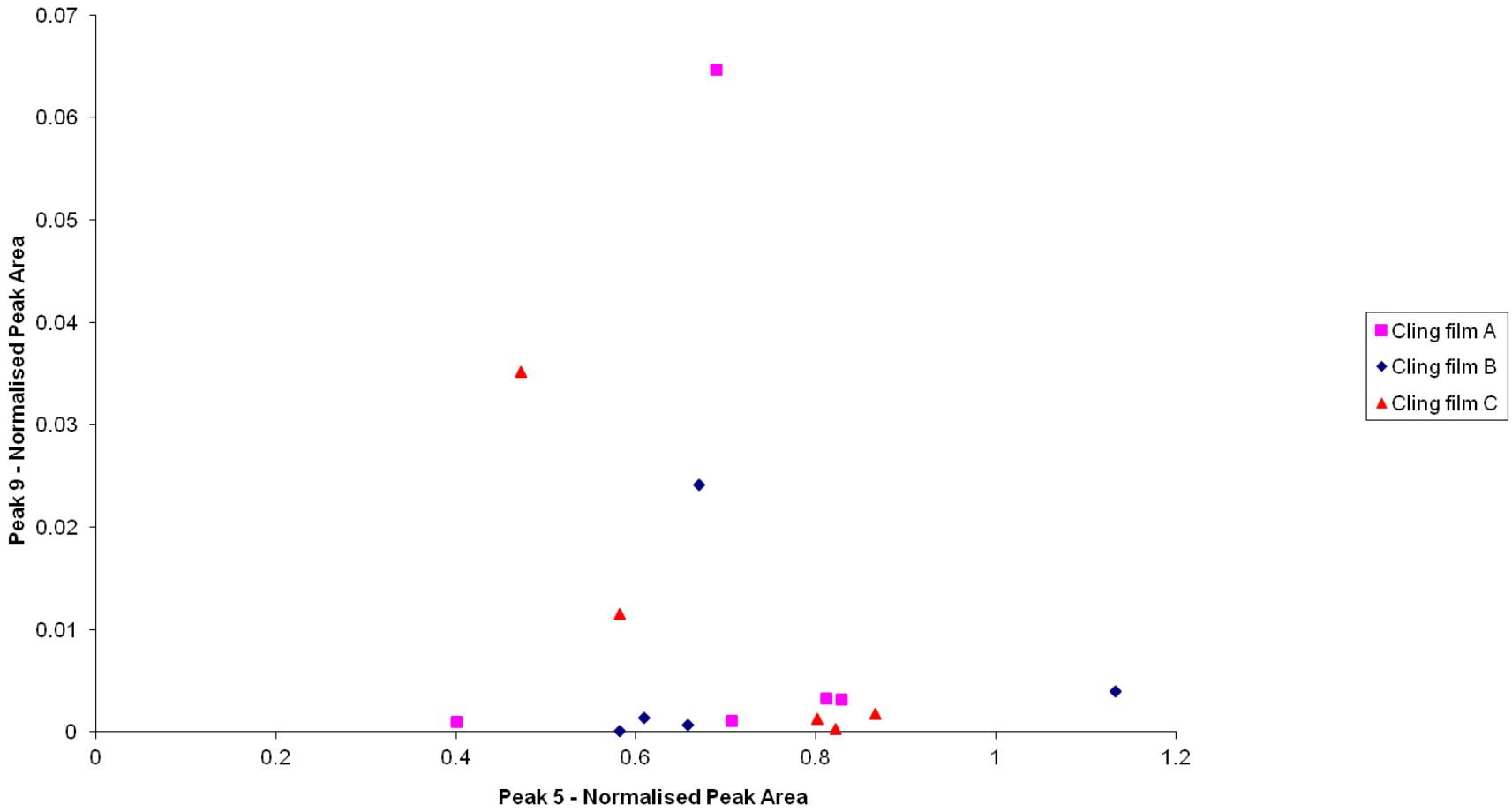

Figure S24 Bivariate plot of the normalised peak areas for peaks 5 and 9 from the five high resolution IR spectra recorded for cling films A, B and C

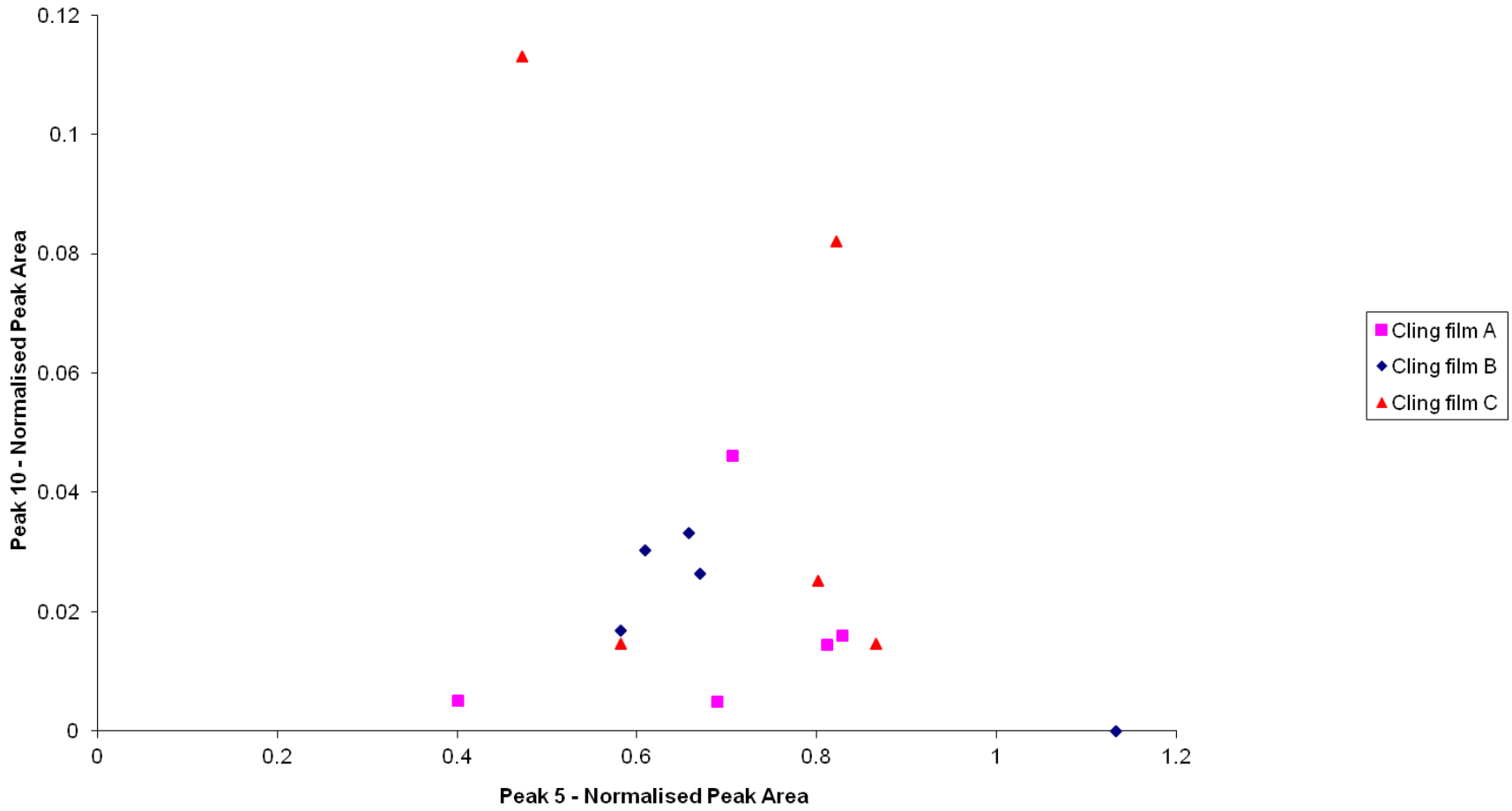

Figure S25 Bivariate plot of the normalised peak areas for peaks 5 and 10 from the five high resolution IR spectra recorded for cling films A, B and C

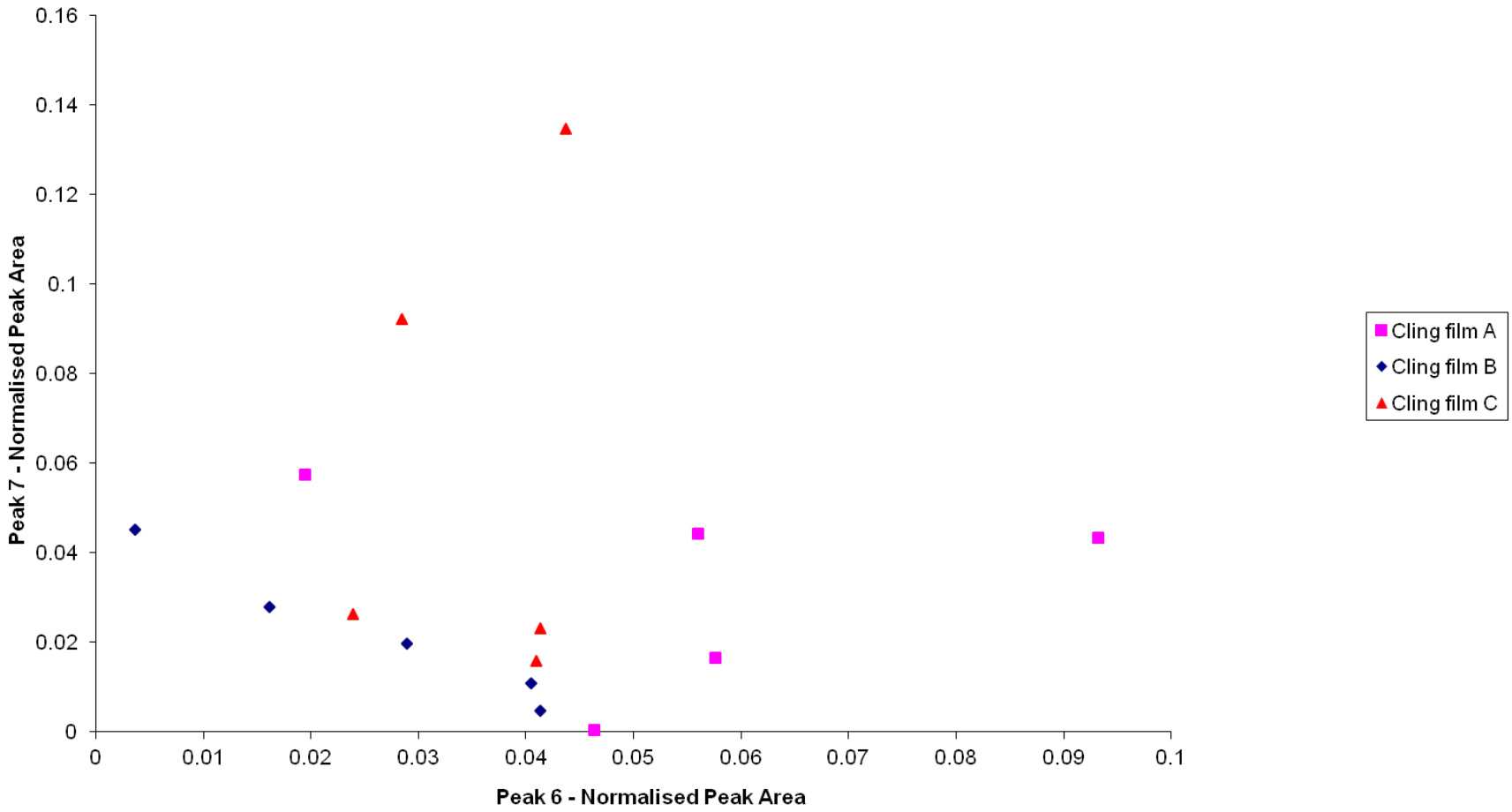

Figure S26 Bivariate plot of the normalised peak areas for peaks 6 and 7 from the five high resolution IR spectra recorded for cling films A, B and C

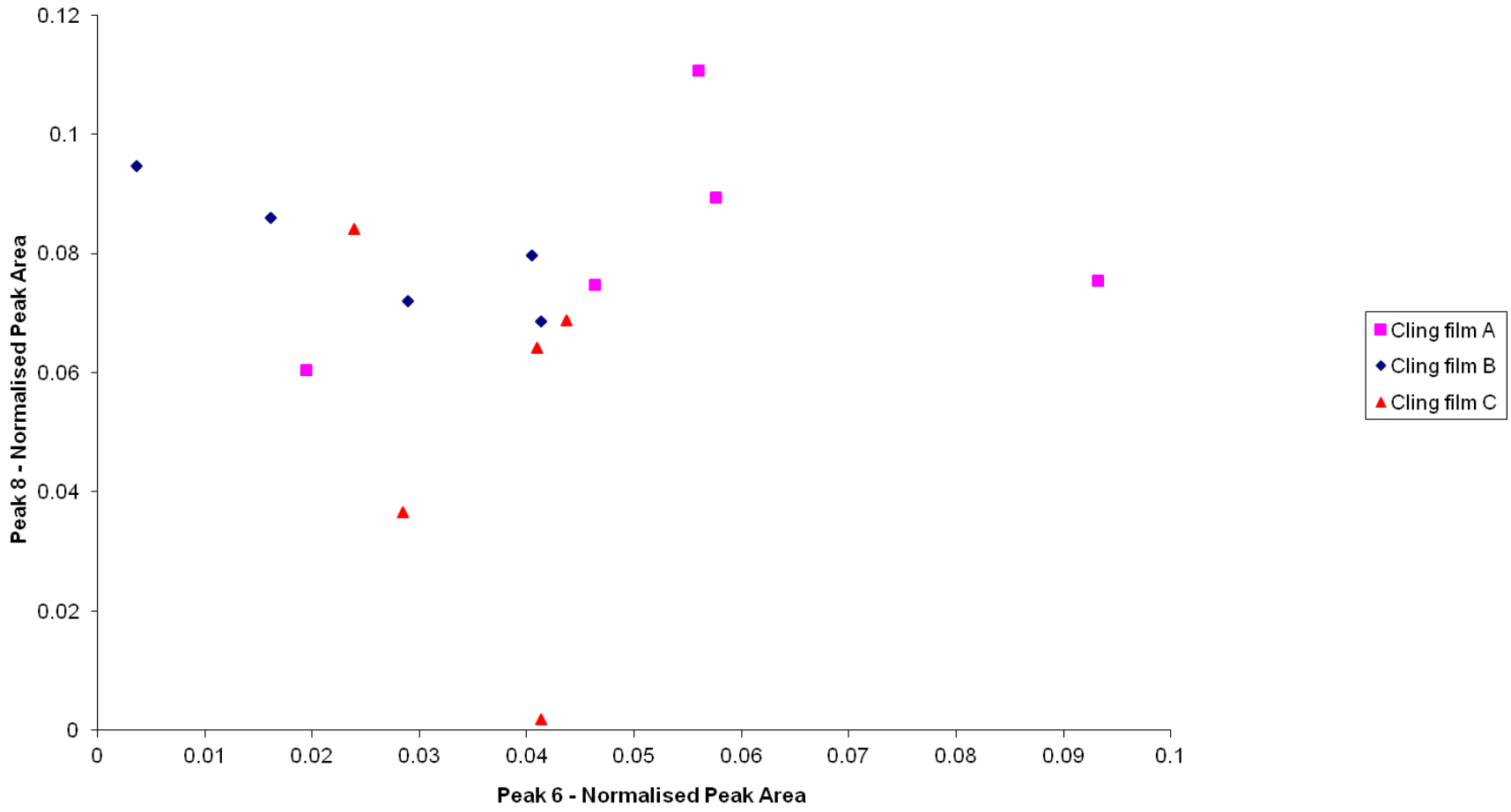

Figure S27 Bivariate plot of the normalised peak areas for peaks 6 and 8 from the five high resolution IR spectra recorded for cling films A, B and C

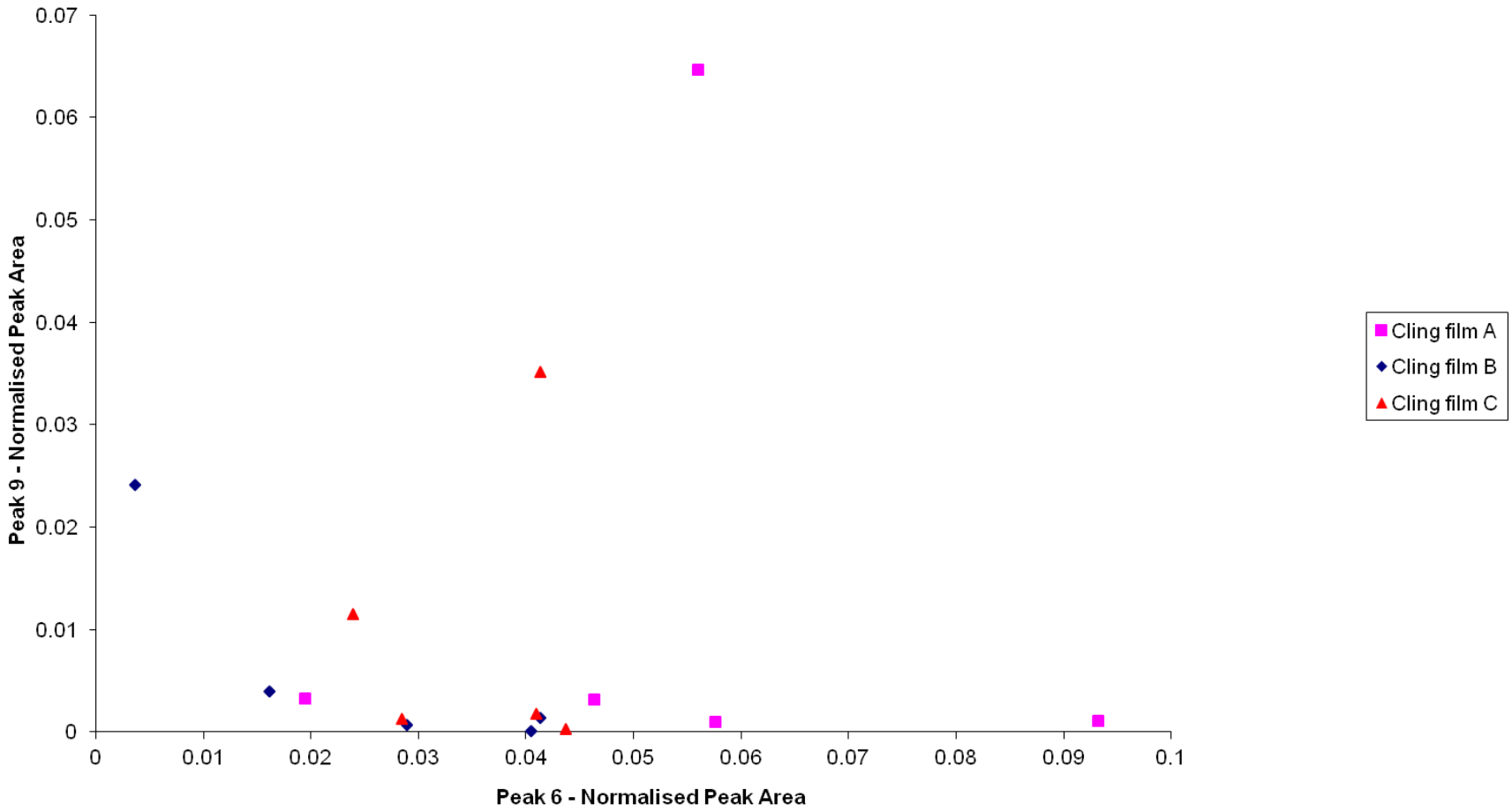

Figure S28 Bivariate plot of the normalised peak areas for peaks 6 and 9 from the five high resolution IR spectra recorded for cling films A, B and C

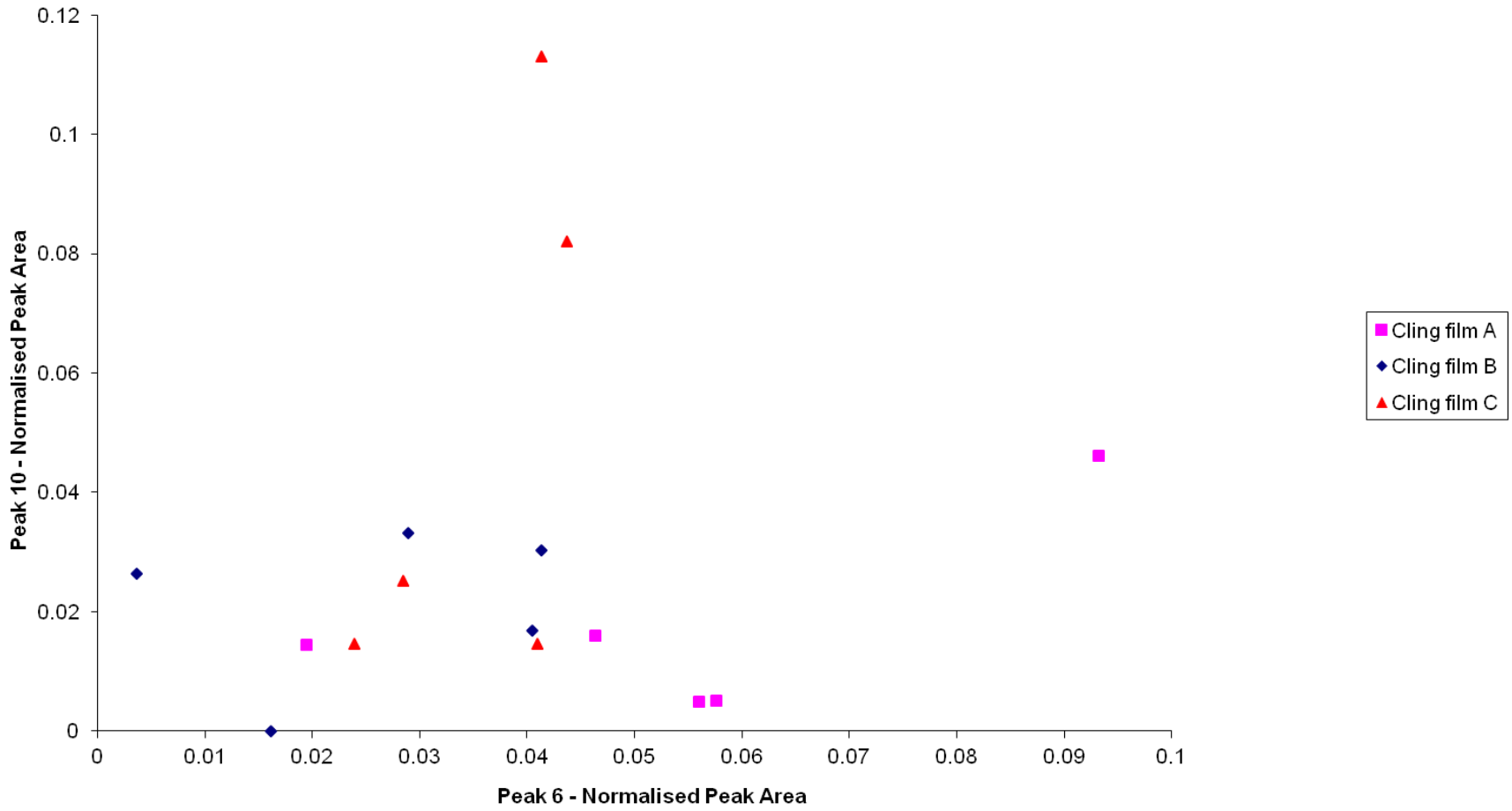

Figure S29 Bivariate plot of the normalised peak areas for peaks 6 and 10 from the five high resolution IR spectra recorded for cling films A, B and C

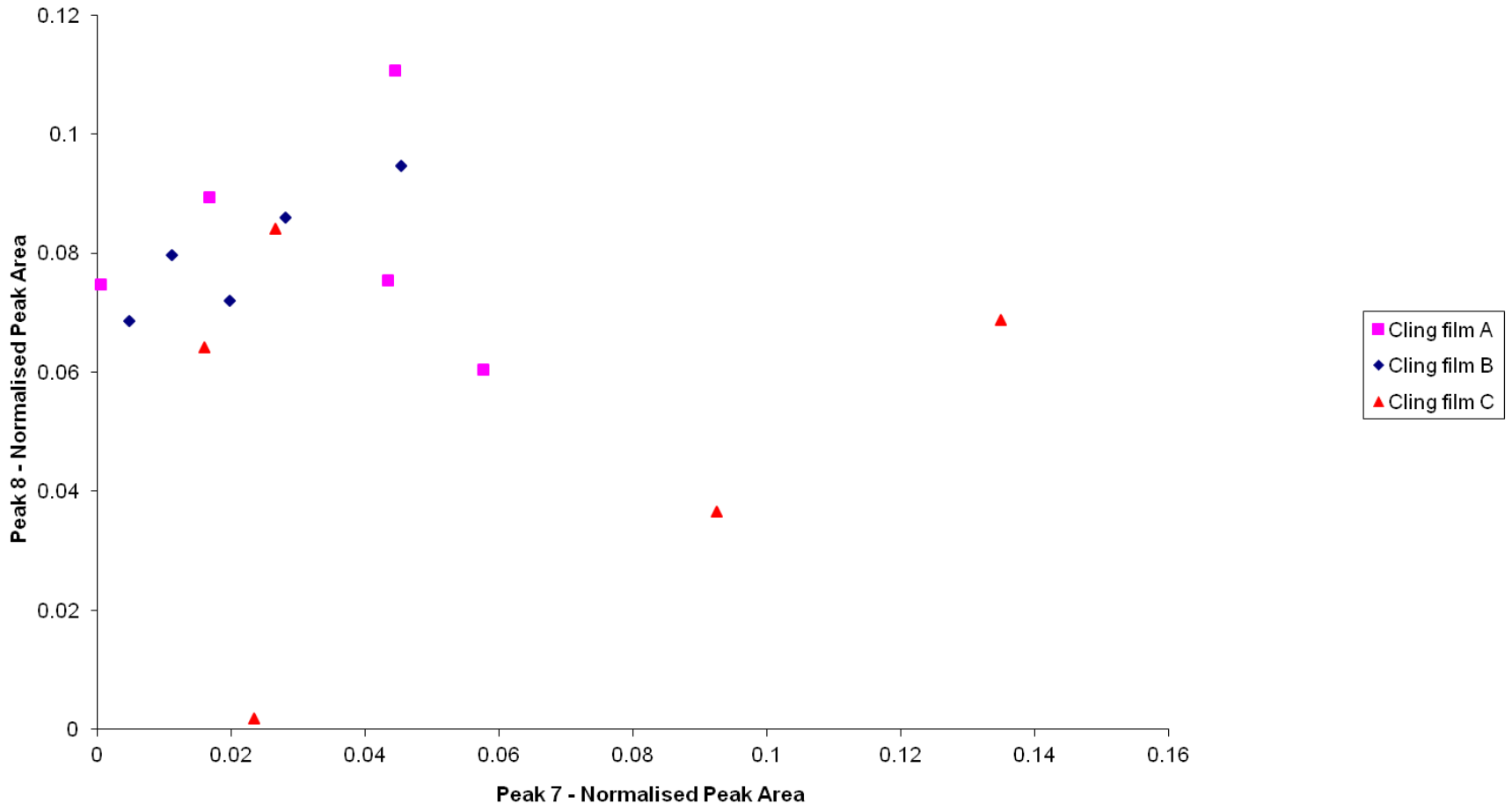

Figure S30 Bivariate plot of the normalised peak areas for peaks 7 and 8 from the five high resolution IR spectra recorded for cling films A, B and C

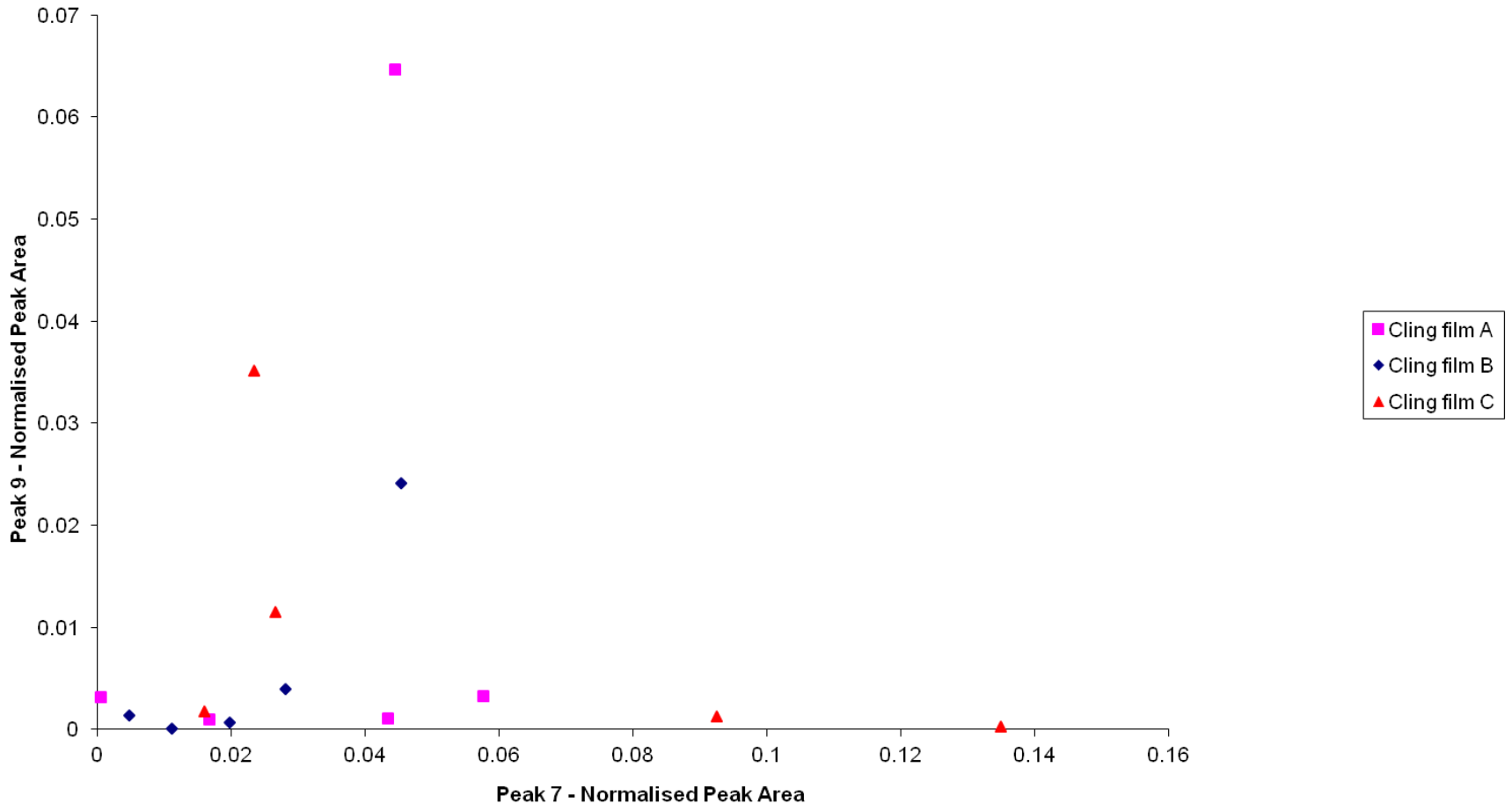

Figure S31 Bivariate plot of the normalised peak areas for peaks 7 and 9 from the five high resolution IR spectra recorded for cling films A, B and C

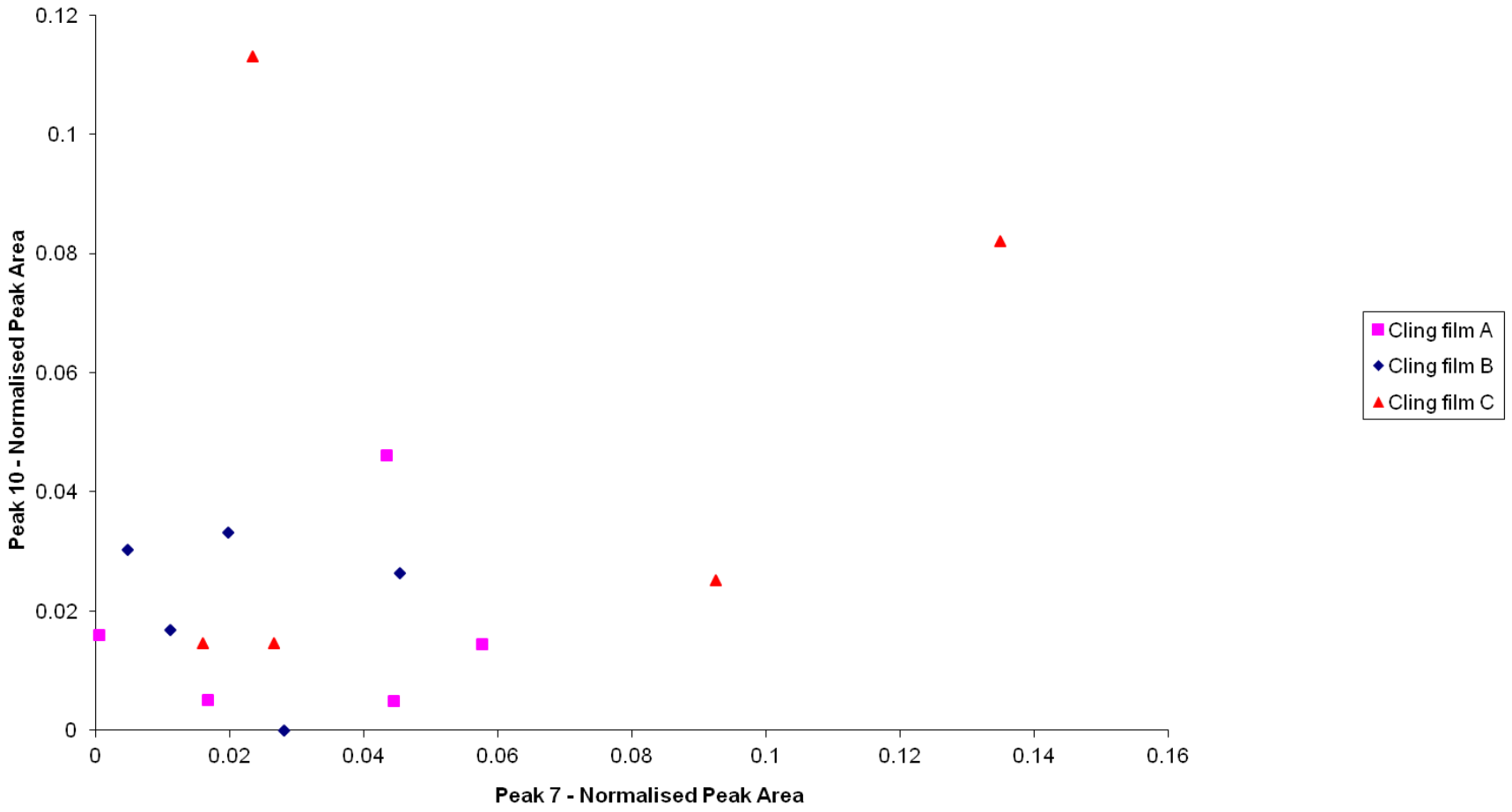

Figure S32 Bivariate plot of the normalised peak areas for peaks 7 and 10 from the five high resolution IR spectra recorded for cling films A, B and C

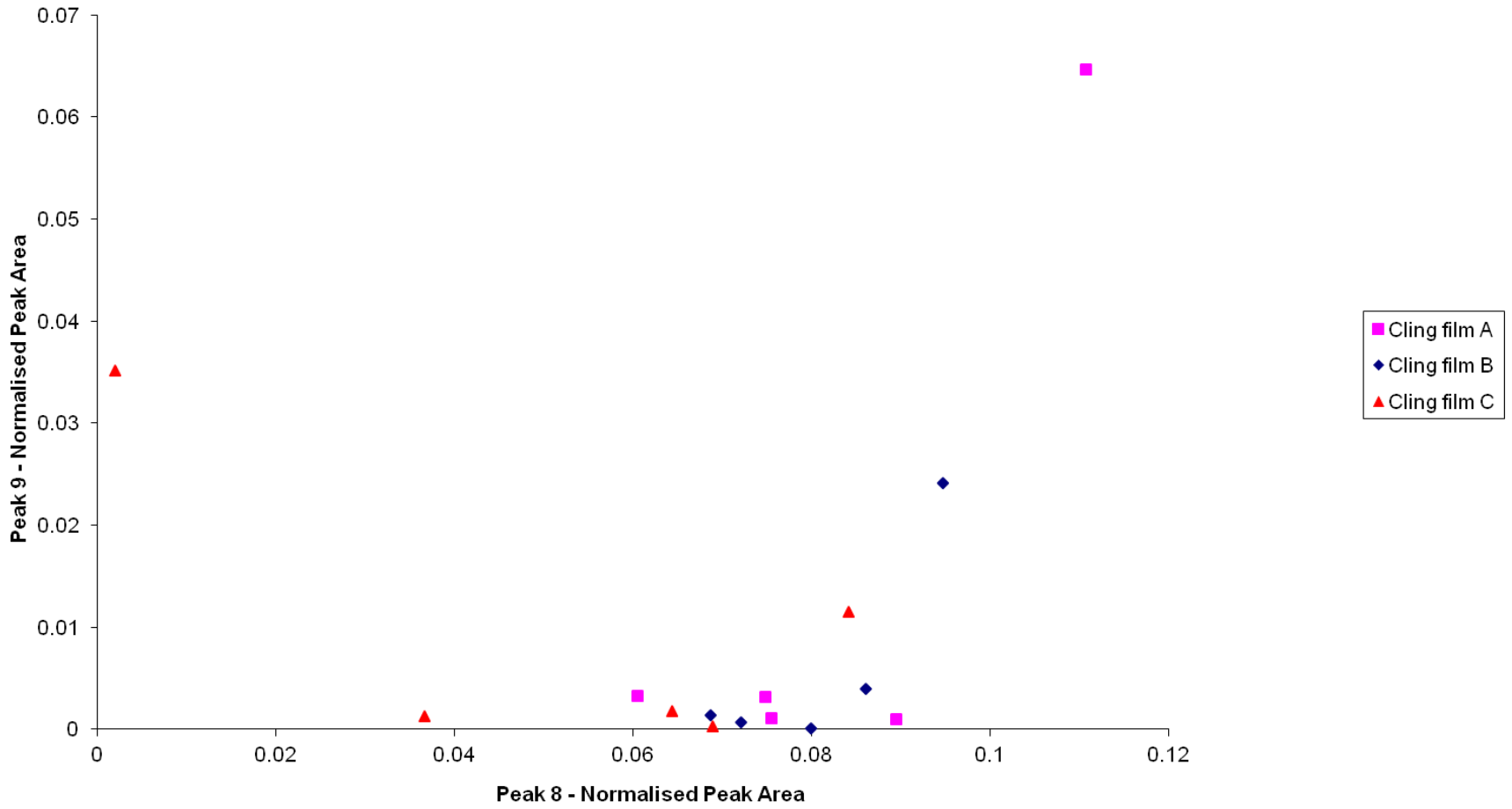

Figure S33 Bivariate plot of the normalised peak areas for peaks 8 and 9 from the five high resolution IR spectra recorded for cling films A, B and C

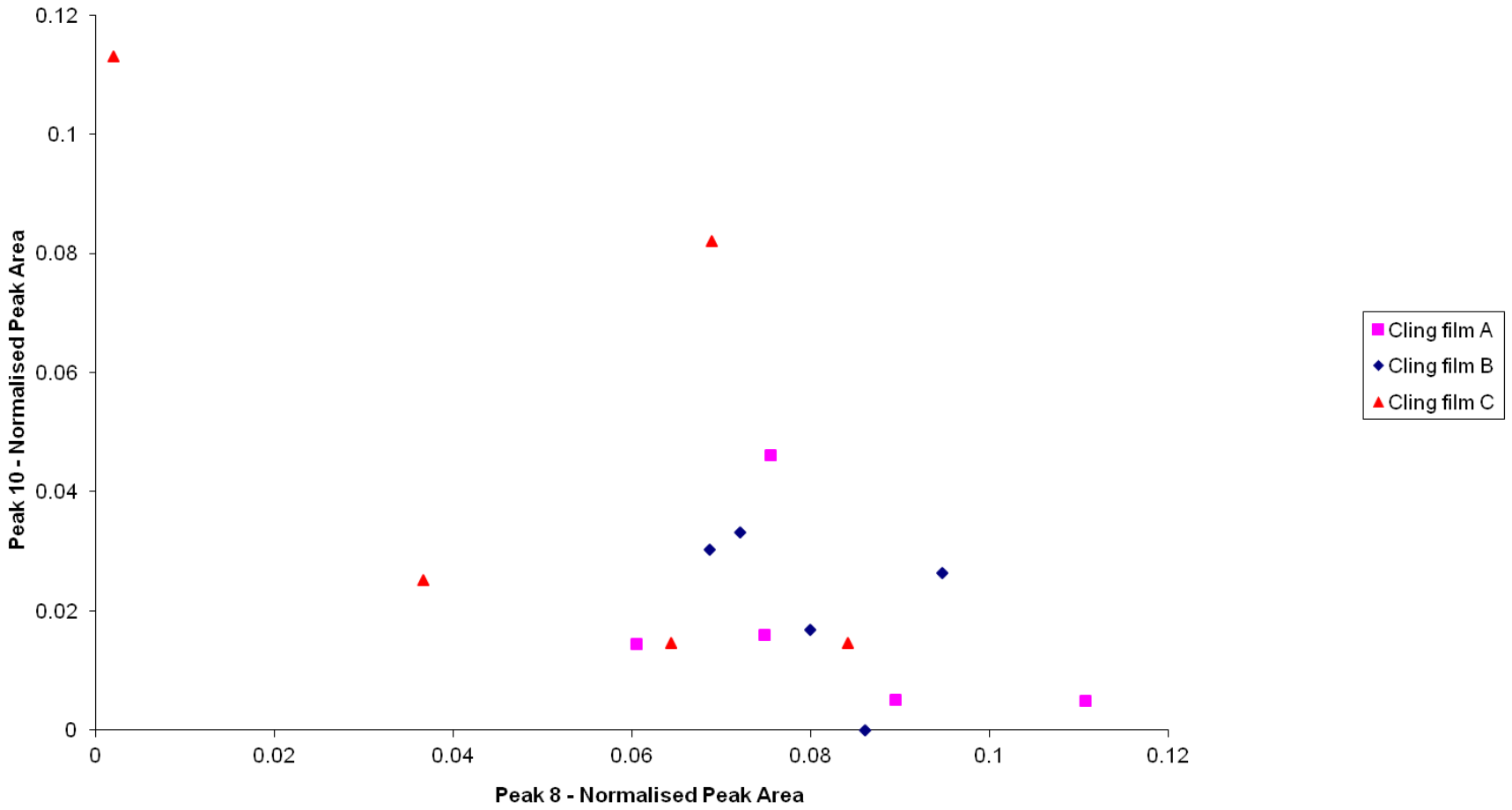

Figure S34 Bivariate plot of the normalised peak areas for peaks 8 and 10 from the five high resolution IR spectra recorded for cling films A, B and C

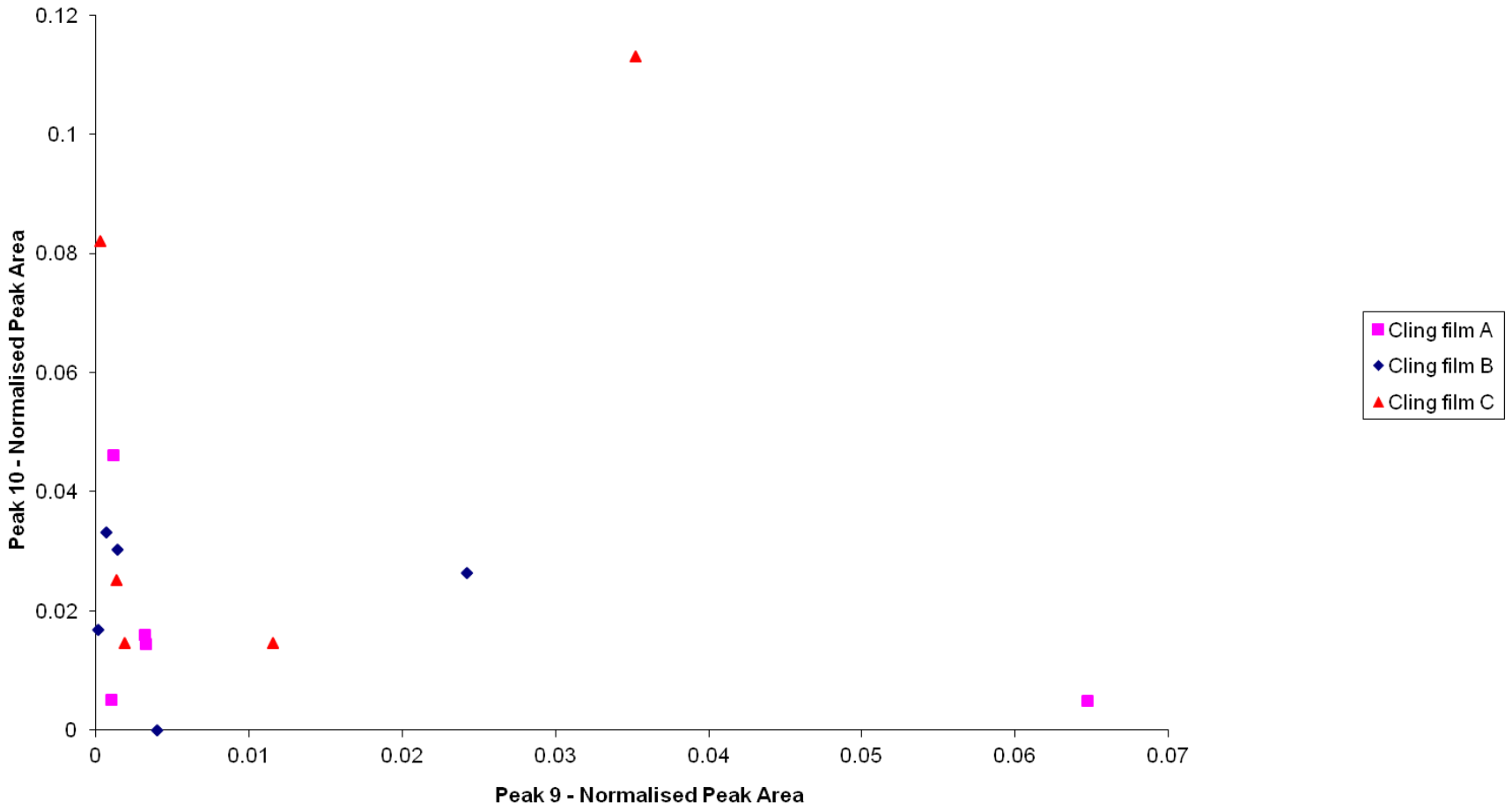

Figure S35 Bivariate plot of the normalised peak areas for peaks 9 and 10 from the five high resolution IR spectra recorded for cling films A, B and C

Table S1 The mean, standard deviation and relative standard deviation of the peak areas of the ten peaks assigned for Cling film A Square 1, Cling film B Square 14 and Cling film C Square 20

Peak number/Reading	**1**	**2**	**3**	**4**	**5**	**6**	**7**	**8**	**9**	**10**
CLING FILM A SQUARE 1										
Mean	17.56	116.27	15.46	46.44	83.34	6.09	3.56	9.49	1.81	1.98
SD	4.03	32.4	4.05	11.5	38.4	2.71	2.79	3.22	3.43	1.68
CV (%)	23.0	27.9	26.2	24.9	46.1	44.5	78.4	33.9	190.0	85.1
CLING FILM B SQUARE 14										
Mean	19.84	126.25	16.30	55.01	87.79	3.43	2.69	10.08	0.71	2.87
SD	6.02	39.5	4.08	29.3	20.1	2.58	1.89	3.13	1.26	1.94
CV (%)	30.4	31.3	25.0	53.3	22.9	75.2	70.5	31.1	178.0	67.7
CLING FILM C SQUARE 20										
Mean	18.71	116.25	15.66	67.64	86.19	4.24	7.00	5.92	0.94	5.44
SD	3.71	34.7	1.86	27.7	42.1	1.78	6.63	3.79	1.38	4.41
CV (%)	19.8	29.9	11.9	41.0	48.9	41.9	94.6	64.0	147.0	81.0